Article

Agonist antibody to guanylate cyclase receptor NPR1 regulates vascular tone

https://doi.org/10.1038/s41586-024-07903-1

Received: 17 April 2023

Accepted: 2 August 2024

Published online: 11 September 2024

Open access

Check for updates

Michael E. Dunn[1]✉, Aaron Kithcart[1], Jee Hae Kim[1], Andre Jo-Hao Ho[1], Matthew C. Franklin[1], Annabel Romero Hernandez[1], Jan de Hoon[2], Wouter Botermans[2], Jonathan Meyer[1], Ximei Jin[1], Dongqin Zhang[1], Justin Torello[1], Daniel Jasewicz[1], Vishal Kamat[1], Elena Garnova[1], Nina Liu[1], Michael Rosconi[1], Hao Pan[1], Satyajit Karnik[1], Michael E. Burczynski[1], Wenjun Zheng[1], Ashique Rafique[1], Jonas B. Nielsen[3], Tanima De[3], Niek Verweij[3], Anita Pandit[3], Adam Locke[3], Naga Chalasani[4], Olle Melander[5,6], Tae-Hwi Schwantes-An[7], Penn Medicine Biobank*, GHS-RGC DiscovEHR Collaboration*, Regeneron Genetics Center*, Aris Baras[3], Luca A. Lotta[3], Bret J. Musser[1], Jason Mastaitis[1], Kishor B. Devalaraja-Narashimha[1], Andrew J. Rankin[1], Tammy Huang[1], Gary Herman[1], William Olson[1], Andrew J. Murphy[1], George D. Yancopoulos[1], Benjamin A. Olenchock[1] & Lori Morton[1]

Heart failure is a leading cause of morbidity and mortality[1,2]. Elevated intracardiac pressures and myocyte stretch in heart failure trigger the release of counter-regulatory natriuretic peptides, which act through their receptor (NPR1) to affect vasodilation, diuresis and natriuresis, lowering venous pressures and relieving venous congestion[3–8]. Recombinant natriuretic peptide infusions were developed to treat heart failure but have been limited by a short duration of effect[9,10]. Here we report that in a human genetic analysis of over 700,000 individuals, lifelong exposure to coding variants of the *NPR1* gene is associated with changes in blood pressure and risk of heart failure. We describe the development of REGN5381, an investigational monoclonal agonist antibody that targets the membrane-bound guanylate cyclase receptor NPR1. REGN5381, an allosteric agonist of NPR1, induces an active-like receptor conformation that results in haemodynamic effects preferentially on venous vasculature, including reductions in systolic blood pressure and venous pressure in animal models. In healthy human volunteers, REGN5381 produced the expected haemodynamic effects, reflecting reductions in venous pressures, without obvious changes in diuresis and natriuresis. These data support the development of REGN5381 for long-lasting and selective lowering of venous pressures that drive symptomatology in patients with heart failure.

Heart failure (HF) remains a progressive and fatal disease, affecting over 64 million people globally[1], with a 50% 5-year survival rate[2]. Several signs and symptoms of HF—pulmonary oedema, pleural effusion and ascites—are manifestations of venous congestion. There is a large unmet need for therapies that durably lower venous pressures and consequently decrease HF hospitalizations and death[11].

Natriuretic peptides (NPs) are a family of prohormones with diverse physiological functions[8] comprising atrial natriuretic peptide (ANP), brain natriuretic peptide (BNP) and c-type NPs. ANP and BNP are released from cardiomyocytes in response to stretch induced by increased pressure or neurohormonal stimuli[3–7]. After release, ANP and BNP are enzymatically cleaved by the proteases corin and furin into active peptides. These active peptides are rapidly degraded, with circulating half-lives of around 30 s and 6.4 min, respectively[12]. The active peptides bind to and signal through a membrane-bound guanylate cyclase, natriuretic peptide receptor 1/A (NPR1, also known as NPRA). NPR1 preferentially binds ANP and BNP and, after agonism, converts intracellular guanosine triphosphate to cyclic guanosine monophosphate (cGMP). NPs are considered to be important regulators of vascular volume and venous tone, and have a critical role in inhibiting the renin–angiotensin–aldosterone system[13,14].

Human genetic variation in *NPR1* has been associated with blood pressure (BP) phenotypes[15–17]. These data establish precedence for NPR1 as a therapeutic target for the modulation of haemodynamics in patients with hypertension, HF and other BP-related diseases. Nevertheless, an association between genetic variation in *NPR1* and HF still needs to be confirmed.

Multiple therapeutic approaches attempting to modulate the NP pathway have been pursued. Several recombinant NPs have been approved for use in patients with HF, including recombinant ANP (carperitide in Japan) and recombinant BNP (nesiritide in the United States; this has since been removed from the market). The dual angiotensin

[1]Regeneron Pharmaceuticals, Tarrytown, NY, USA. [2]Center for Clinical Pharmacology, University Hospitals Leuven, Leuven, Belgium. [3]Regeneron Genetics Center, Regeneron Pharmaceuticals, Tarrytown, NY, USA. [4]Indiana University School of Medicine & Indiana University Health, Indianapolis, IN, USA. [5]The Department of Clinical Sciences Malmö, Lund University, Malmö, Sweden. [6]Department of Emergency and Internal Medicine, Skåne University Hospital, Malmö, Sweden. [7]Department of Medical and Molecular Genetics, Indiana University School of Medicine, Indianapolis, IN, USA. *Lists of authors and their affiliations appear at the end of the paper. ✉e-mail: michael.dunn@regeneron.com

a

Exposure	Outcome	*n* (ref./het./alt.)	*β* (95% CI)	Unit	*P*	Freq. (%)
NPR1:p.Glu967Lys, rs35479618 (LOF)	Systolic blood pressure	658,975/21,263/197	1.13 (0.92 to 1.33)	mm Hg	1.3×10^{-26}	3.16
	Diastolic blood pressure	658,545/21,248/197	0.59 (0.47 to 0.71)	mm Hg	1.1×10^{-21}	3.16
	NT-proA	77,021/2,554/18	188.84 (50.98 to 326.71)	pg ml^{-1}	0.0073	3.23
NPR1:p.Leu1034Phe, rs116245325 (LOF)	Systolic blood pressure	667,895/1,034/1	2.49 (1.55 to 3.42)	mm Hg	1.9×10^{-7}	0.15
	Diastolic blood pressure	667,445/1,039/1	1.29 (0.74 to 1.83)	mm Hg	3.5×10^{-6}	0.16
	NT-proBNP	76,300/121/0	1,058.14 (415.17 to 1,701.10)	pg ml^{-1}	0.0013	0.16
NPR1:p.Gly541Ser, rs61757359 (GOF)	Systolic blood pressure	674,628/4,610/8	−0.95 (−1.39 to −0.51)	mm Hg	2.8×10^{-5}	0.68
	Diastolic blood pressure	674,194/4,599/8	−0.56 (−0.82 to −0.30)	mm Hg	2.0×10^{-5}	0.68
	NT-proBNP	78,258/531/0	−182.65 (−483.00 to 117.71)	pg ml^{-1}	0.233	0.67
NPR1 protein-truncating variants, freq. <1%	Systolic blood pressure	680,142/558/0	1.85 (0.57 to 3.14)	mm Hg	0.0047	0.08
	Diastolic blood pressure	679,696/559/0	0.63 (−0.11 to 1.38)	mm Hg	0.097	0.08
	NT-proBNP	78,195/85/0	818.95 (68.04 to 1,569.86)	pg ml^{-1}	0.033	0.11

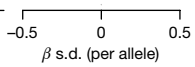

b

Exposure	Outcome	*n* (ref./het./alt.)	*β* (95% CI)	Unit	*P*	Freq. (%)
NPR1 LOF variants, freq. <1%	Systolic blood pressure	307,842/10,886/89	1.24 (0.95 to 1.52)	mm Hg	3.9×10^{-17}	3.44
	Diastolic blood pressure	307,689/10,886/89	0.70 (0.54 to 0.87)	mm Hg	2.5×10^{-16}	3.44
	NT-proBNP	45,287/1,631/10	165.07 (34.38 to 295.76)	pg ml^{-1}	0.013	3.49
NPR1 GOF variants, freq. <1%	Systolic blood pressure	316,004/2,287/5	−0.83 (−1.46 to −0.21)	mm Hg	0.0089	0.72
	Diastolic blood pressure	315,858/2,280/5	−0.55 (−0.92 to −0.19)	mm Hg	0.0031	0.72
	NT-proBNP	46,091/323/0	−298.12 (−584.22 to −12.03)	pg ml^{-1}	0.041	0.69

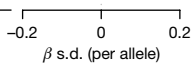

c

Exposure	Outcome	*n* (ref./het./alt.)	OR (95% CI)	*P*	Freq. (%)
NPR1 LOF variants, freq. <1%	Heart failure	Case: 44,853/1,510/13 Control: 219,175/7,236/61	1.07 (1.01 to 1.14)	0.034	3.23
NPR1 GOF variants, freq. <1%	Heart failure	Case: 46,066/309/1 Control: 224,773/1,695/4	0.91 (0.79 to 1.04)	0.154	0.74

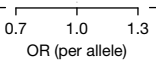

Fig. 1 | Protein-altering genetic variants in *NPR1* and the associated effect on BP and NT-proBNP in 718,386 individuals. a, We replicated three previously reported and functionally validated missense variants with a known effect on BP[15]. Two reported LOF variants (*NPR1*:p.L1034F-rs116245325 and *NPR1*:p.G967K-rs35479618) were associated with increased BP and higher NT-proBNP, while a reported GOF variant (*NPR1*:p.G541S-rs61757359) was associated with lower BP and directionally lower NT-proBNP. We also found that individuals carrying a protein-truncating variant (presumed LOF) of *NPR1* on average have higher BP and higher NT-proBNP than that of non-carriers. **b**, We defined any protein-altering variant associated with increased BP as presumed LOF ($n = 9$) and any BP-decreasing protein-altering variant as presumed GOF ($n = 5$). In an independent sample, we found that the combined collection of presumed LOF variants is associated with increased BP and higher NT-proBNP, while the collection of presumed GOF variants is associated with decreased BP and lower NT-proBNP. **c**, The collection of presumed LOF variants is associated with increased odds of HF, while the collection of presumed GOF variants is numerically associated with a decreased odds of HF, based on an additive genetic model performed in independent samples. Alt., alternative allele; CI, confidence intervals; freq., frequency; het., heterozygous allele; OR, odd ratio; ref., reference allele.

receptor blocker and neprilysin inhibitor sacubitril/valsartan is an indirect activator of the NP pathway and was approved in 2015 for patients with HF with reduced ejection fraction[18] and in 2021 for patients with HF with preserved ejection fraction[19]. Recombinant ANP infusion in healthy volunteers decreased preload and pulmonary capillary wedge pressure (PCWP). Consistent with Frank–Starling predictions[20], ANP-induced reductions in preload to below normal in a healthy heart was associated with decreased stroke volume, increased heart rate and reduced systolic BP[19]. Conversely, as also predicted by Frank–Starling, in patients with congested HF who have abnormally high preload, a marked decrease in PCWP observed after ANP infusion was associated with increased stroke volume and cardiac output[19]. These data provide strong evidence for the critical role of NPR1 in modulating venous pressure, and provide the therapeutic rationale for a long-lasting NPR1 agonist that obviates the need for continuous infusion, while still improving cardiac function in HF.

We conducted a high-throughput screen, using VelocImmune technology, to identify REGN5381, which is an investigational human immunoglobulin G4-based monoclonal antibody that binds to and directly activates NPR1 in the presence or absence of endogenous ligands. Signalling directly through NPR1 using an agonist antibody may enable many of the beneficial physiological responses seen with other NP pathway therapeutics, including preferential venous pressure reduction, but with added selectivity, potency and enhanced durability. We report the generation, preclinical characterization and first-in-human evaluation of an investigational agonist monoclonal antibody, REGN5381, that selectively binds to and agonizes NPR1.

Human genetic validation of *NPR1* in HF

We performed genetic analysis, using sequencing data produced by the Regeneron Genetics Center, to confirm and extend insights into lifelong genetic modulation of NPR1 function. In 718,386 individuals from 6 cohorts and 5 ancestry groups with exome sequencing data (Supplementary Table 1), we first confirmed that two previously reported and functionally validated loss-of-function (LOF) variants (*NPR1*:p.E967K and *NPR1*:p.L1034F)[15,17] were associated with higher BPs, while, conversely, a previously reported and functionally validated gain-of-function (GOF) variant (*NPR1*:p.G541S) was associated with lower BPs (Fig. 1a). We extended these observations by showing that the two previously reported LOF variants were also associated with higher levels of a biomarker of HF (N-terminal pro B-type natriuretic peptide (NT-proBNP)), while the GOF variant was associated with

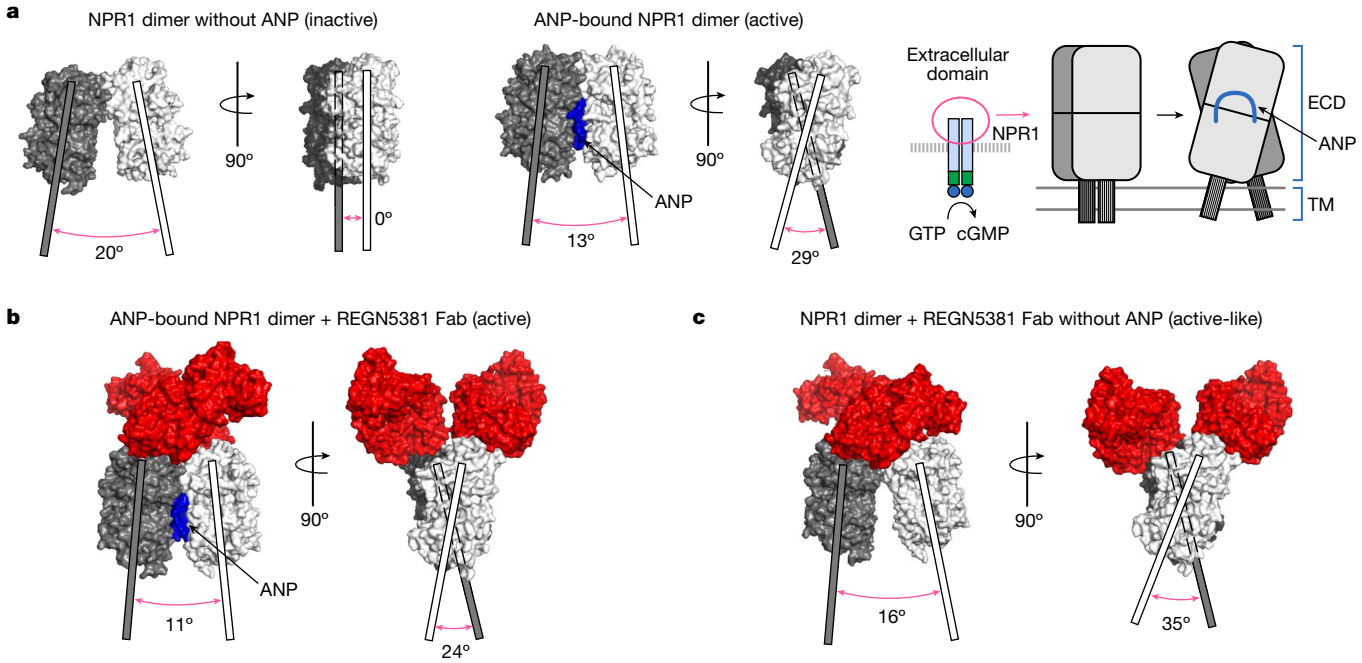

Fig. 2 | The cryo-EM structure of antibody-bound NPR1 suggests that REGN5381 is an allosteric activator. a, The extracellular domains of an inactive ANP-free NPR1 dimer (PDB: 1DP4) are shown in two different orientations as a molecular surface, one monomer in white and the other monomer in dark grey, with the principal axes of each monomer indicated as thick solid white or grey lines, respectively; the projection angle between the axes is indicated below the monomers. The active, ANP-bound NPR1 dimer (PDB: 1T34) is shown similarly to the diagram at left, as a blue surface for bound ANP. The same complexes are shown in schematic form (extracellular domain, transmembrane helix, ANP) on the right, including possible positions for the transmembrane helices. **b**, The NPR1–ANP–REGN5381 complex is shown similarly to **a**. **c**, The NPR1–REGN5381 complex is shown similarly to **a**, with the addition of REGN5381 Fab molecular surface in red.

non-significantly numerically lower levels of this biomarker (Fig. 1a). We also showed that an independent set of NPR1 protein-truncating variants (presumed LOF) were also associated with increased BP and levels of NT-proBNP (Fig. 1a). Moreover, we derived a collection of nine presumed LOF and five presumed GOF coding variants on the basis of their association with BP. In independent samples, the burden of BP increasing presumed-LOF variants was associated with higher NT-proBNP and increased odds of HF, whereas the burden of BP-lowering presumed-GOF variants was associated with lower NT-proBNP and non-significantly numerically lower odds of HF (Fig. 1b,c and Supplementary Table 2). Taken together, these data are supportive of a beneficial role of long-term agonism of NPR1 in the setting of HF.

In vitro characterization of REGN5381

We conducted a broad-scale in vitro screen and identified the best NPR1-activating antibody, REGN5381, using VelocImmune technology[21,22]. REGN5381 binds to cells expressing human NPR1 (hNPR1) and monkey NPR1 (mfNPR1) in the absence of ligands, and binding is enhanced in the presence of ANP and BNP (Extended Data Fig. 1a–c). Biacore data confirmed that REGN5381 binds to the extracellular domain protein of hNPR1 and mfNPR1 in the presence or absence of ANP or BNP, but not to the mouse NPR1 protein (Supplementary Table 3). REGN5381 binding is specific to NPR1, displaying no binding to NPR2 and NPR3 (Supplementary Table 4). A summary of REGN5381 antigen-binding fragment (Fab) residues interacting with NPR1 residues in the REGN5381–NPR1–ANP complex is shown in Supplementary Table 5. Furthermore, REGN5381 does not interact with ANP or block the binding of ANP to NPR1 (Extended Data Fig. 2).

Activation of NPR1 signalling by REGN5381 was demonstrated in a Ca^{2+} flux bioassay in which cGMP production, through NPR1 agonism, was coupled with the opening of cyclic-nucleotide-gated calcium channels, CNGA2[23] (Extended Data Fig. 1d). REGN5381 agonizes hNPR1 and mfNPR1 in the absence or presence of ANP or BNP, with the maximum activation comparable to the level achieved by ligand but at high concentrations of the antibody (Extended Data Fig. 1e,f). Moreover, REGN5381 bound to and activated canine NPR1, with a 50% of the maximal response (EC_{50}) value of >100 nM (Supplementary Fig. 1). To confirm the level of activation in a direct measurement of cGMP produced by cells, a homogeneous time-resolved fluorescence (HTRF) cGMP assay was performed. A dose-dependent accumulation of cGMP by REGN5381 was observed, with a lower maximum level of activation than that achieved by ANP or BNP alone. The HTRF assay also revealed enhanced activation in the presence of ANP or BNP (Extended Data Fig. 3). Taken together, these results show that REGN5381 can bind to and activate NPR1 directly without ligand, binding activation can be enhanced in the presence of ligand and the maximum activation achieved is comparable with or lower than the maximum activation achieved by ligand, depending on the activation assay.

Structural biology and epitope mapping

NPR1 has been previously shown to form a dimer that undergoes a conformational change after ANP binding, in which one monomer's extracellular domain rotates relative to the other[24,25] (Fig. 2a). We used cryo-electron microscopy (cryo-EM) to examine complexes of NPR1 ectodomain bound to REGN5381, in the presence and absence of ANP, to determine whether similar structural changes were occurring. A cryo-EM structure of the NPR1 ectodomain bound to ANP as well as the Fab of REGN5381 showed that REGN5381 bound to the top of the N-terminal domain of NPR1, more than 25 Å distant from ANP, which is held in the centre of the NPR1 dimer (Fig. 2b and Supplementary Fig. 2). Two REGN5381 Fabs are bound in this complex, one per NPR1 monomer. Details of REGN5381-Fab interactions are provided in Supplementary Table 3. The NPR1–ANP–REGN5381 complex adopts an active conformation of the NPR1 dimer comparable to the NPR1–ANP crystal structure

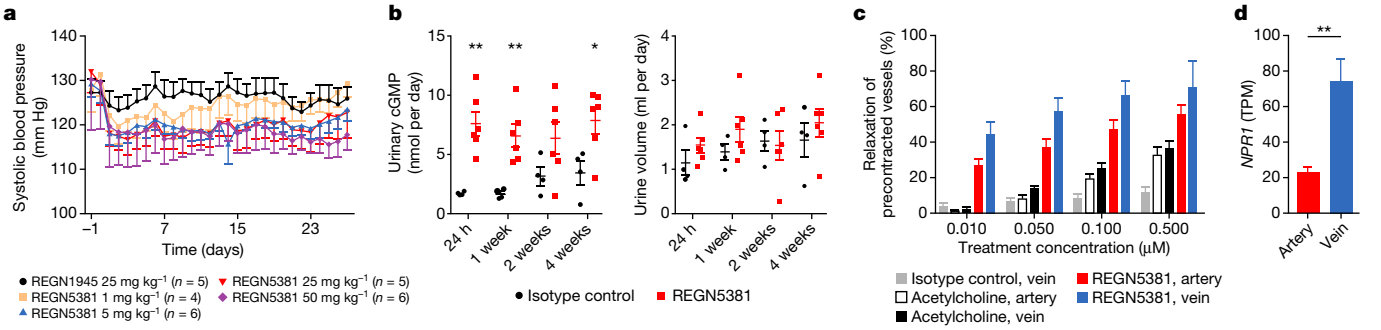

Fig. 3 | The NPR1 agonist antibody REGN5381 persistently reduces systolic BP in *NPR1*$^{hu/hu}$ mice in the absence of diuresis, and acts as a direct vasodilator. **a**, Administration of a single subcutaneous dose of 1, 5, 25 or 50 mg per kg REGN5381 in normotensive *NPR1*$^{hu/hu}$ mice demonstrated marked reductions in systolic BP that were maintained for up to 28 days (black circles, REGN1945 (the immunoglobulin G4 isotype control), 25 mg per kg; pink squares, REGN5381, 1 mg per kg; blue triangles, REGN5381, 5 mg per kg; red triangles, REGN5381, 25 mg per kg; purple diamonds, REGN5381, 50 mg per kg). **b**, Post-dose assessments after administration of REGN5381 (red squares) or control monoclonal antibody (REGN1945; black circles) on urinary cGMP concentration and urine volume. **c**, Administration of REGN5381 induces greater venous dilation in precontracted ex vivo vessels from *NPR1*$^{hu/hu}$ mice, as evaluated in an ex vivo vessel ring assay (grey bars, isotype control, vein; black bars, acetylcholine, vein; white bars, acetylcholine, artery; blue bars, REGN5381, artery; red bars, REGN5381, vein). **d**, *NPR1* expression is significantly higher in the femoral vein than in the femoral artery.

(Protein Data Bank (PDB): 1T34)[24]. Cryo-EM data are shown in Extended Data Table 1, and the activity of REGN5381 and ligand at hNPR1 is shown in Fig. 2a,c. There were no significant changes to the NPR1 monomer conformation after REGN5381 binding; a superposition of one NPR1 monomer from this structure with one from PDB 1T34 shows a 1.03 Å Cα root mean squared deviation overall, with only two residues (Pro42 and Gly43) shifting by more than 2 Å. Asymmetric flow field-flow fractionation coupled to multi-angle light scattering (A4F-MALS) experiments provided data consistent with this structure, demonstrating that more than one REGN5381 IgG can bind to an NPR1 dimer, and suggesting that both Fab arms of the REGN5381 antibody are unable to bind to a single NPR1 dimer (Supplementary Fig. 2).

We next produced a cryo-EM structure of the complex of NPR1 with REGN5381 without ANP bound (Fig. 2c and Extended Data Fig. 4). The EM density for this structure is substantially lower, probably due to the greater flexibility of the NPR1 dimer without ANP to stabilize it. However, we can clearly see that the complex adopts an active-like state (Fig. 2c), with NPR1 intermonomer angles similar to those of the ANP-bound active state (Fig. 2b), even though there is no density for any bound peptide at the ANP-binding site (Extended Data Fig. 4). This active-like state is probably maintained by the presence of the two REGN5381 Fabs.

REGN5381 in normotensive *NPR1*$^{hu/hu}$ mice

We next wanted to confirm that REGN5381 would have the expected BP-lowering effects in animal studies. The fully human antibody REGN5381 is selective to hNPR1 (and mfNPR1 and canine), but does not bind to the mouse NPR1 protein; we therefore genetically humanized NPR1 to facilitate functional characterization of REGN5381 in mice. Mice were genetically engineered to express the hNPR1 extracellular domain, with the mouse transmembrane and intracellular aspects preserved (NPR1 humanized mice; called '*NPR1*$^{hu/hu}$ mice' here). Telemetered normotensive *NPR1*$^{hu/hu}$ mice receiving a single subcutaneous dose of 1, 5, 25 or 50 mg per kg REGN5381 demonstrated a 10–15 mm Hg reduction in systolic BP, maintained throughout the 28-day study period (Fig. 3a and Supplementary Fig. 3). The duration of the effect was dose dependent, with a loss of BP effect in the 1 mg per kg dose group after 10 days, moderate effects of 5 and 25 mg per kg after approximately 3 weeks, and a persistent effect of a single 50 mg per kg high dose until the end of the observation period. There was no apparent difference in the magnitude of BP reduction between the 5 and 25 mg per kg dose groups, indicating that 5 mg per kg is a saturating dose. The maximum BP reductions pharmacologically achieved using REGN5381 are about half of those achieved using constant high-dose ANP and BNP delivery through hydrodynamic DNA delivery in mice (Extended Data Fig. 5). Relative to standard-of-care HF and hypertension agents, REGN5381 reduced systolic BP to similar levels, with additive effects observed after combination with some but not all agents; the greatest additive effect was observed when combined with an angiotensin-converting enzyme inhibitor or angiotensin receptor blocker (Extended Data Fig. 6). Consistent with the robust reductions in systolic BP due to REGN5381-mediated activation of the guanylate cyclase receptor NPR1, we observed a significant increase in urinary cGMP (Fig. 3b); despite published observations that NPs can cause diuresis, post-dose evaluation of urine output after ANP or REGN5381 administration could not demonstrate effects on urine output (Fig. 3b; other data are not shown).

Precontracted ex vivo vessels from mice

To confirm that REGN5381 is working like the endogenous NP ligands and induces the reported preferential venodilatory effects[14], we evaluated REGN5381 in an ex vivo vessel ring assay to assess whether there was a differential effect on arterial or venous tone. Vascular function effects of REGN5381 were evaluated in vessels (aorta, mesenteric artery, mesenteric vein, pulmonary artery, pulmonary vein) that were isolated from *NPR1*$^{hu/hu}$ mice and preconstricted with phenylephrine. REGN5381 induced vasodilation of both arterial and venous vessels (Fig. 3c) with superior potency relative to control agent, acetylcholine; however, in contrast to acetylcholine, for which the magnitude of effect was similar on both arterial and venous vessels, REGN5381 showed the largest effect on venous vessels. Consistent with the vasodilatory effects of REGN5381, gene expression analysis shows that *NPR1* is expressed at much higher levels in veins than in arteries (Fig. 3d).

REGN5381 in anaesthetized canines

Owing to the difficulty in measuring central venous pressure (CVP) in mice, we used the standardized canine model to confirm that REGN5381 would lower CVP similarly to native NPs[26], which was enabled by our demonstration that REGN5381 engages canine NPR1 (Supplementary Fig. 1). We first showed that, as in humanized mice, a single intravenous 25 mg per kg dose of REGN5381 lowered systolic BP and increased urinary cGMP levels in beagle canines (Fig. 4a,b). We then conducted an acute haemodynamic study showing that REGN5381 reduced CVP and pulmonary arterial pressure and resulted in compensatory heart rate

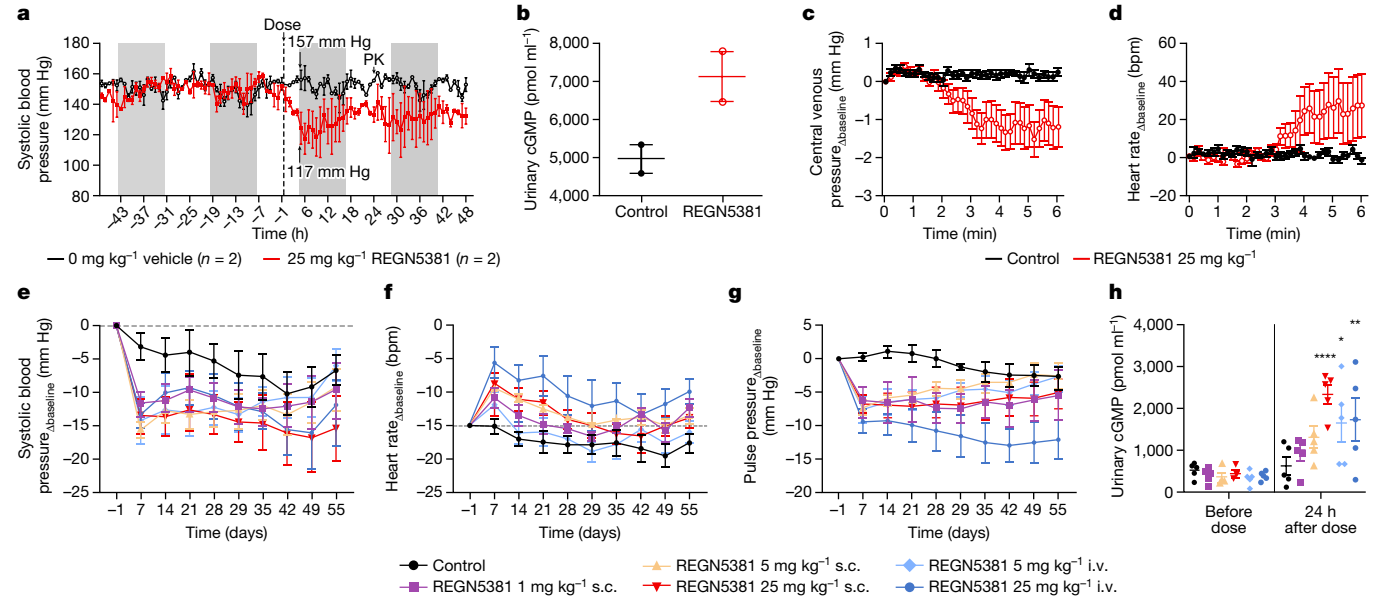

Fig. 4 | REGN5381 reduces systolic BP and CVP in a temporally dose-dependent manner. a,**b**, Beagle canines were surgically implanted with a radiotelemetry transmitter. A cross-over design was used and animals each received a single intravenous bolus of saline (control) ($n = 2$; black circles) or REGN5381 25 mg per kg ($n = 2$; red circles). BP measurements were collected pre-dose (baseline measurements) and during a 48 h post-dose monitoring period. Post-dose systolic BP assessment after administration of REGN5381 (red circles) or control (saline, black circles) (**a**) and urinary cGMP concentration (**b**). PK, pharmacokinetics. **c**,**d**, Anaesthetized beagle canines were instrumented with venous and arterial catheters. Each canine received a single intravenous bolus of saline (control, $n = 6$) or 25 mg per kg REGN5381 ($n = 6$) and was monitored for acute haemodynamic changes. Post-dose CVP (**c**) and heart rate (**d**) change from baseline (subscripted 'Δbaseline') is shown. bpm, beats per minute. **e**–**h**, Cynomolgus monkeys were surgically implanted with a radiotelemetry transmitter. The animals each received a single intravenous bolus of saline/vehicle ($n = 4$; black circles) or REGN5381 subcutaneously (s.c.; $n = 4$, 1 mg per kg, pink line; $n = 5$, 5 mg per kg, pale yellow line; $n = 5$, 25 mg per kg, red line) or intravenously ($n = 5$, 5 mg per kg, light blue line; $n = 5$, 25 mg per kg, dark blue line). BP measurements were collected for each animal before dosing (baseline measurements) and until study day 56. The change from baseline over time was determined for each individual non-human primate (NHP) for systolic BP (**e**), heart rate (**f**) and pulse pressure (**g**). **h**, The baseline and 24 h post-dose cGMP levels in the urine of non-human primates. Each symbol represents one individual animal. Data are mean ± s.e.m. *$P = 0.0178$ (light blue group), **$P = 0.0081$ (dark blue group), ****$P < 0.0001$ (red group).

elevation in anaesthetized, supine-positioned beagle canines with implanted central venous Swan–Ganz catheters (Fig. 4c,d and Supplementary Fig. 4), analogously to what has been shown for ANP in healthy human volunteers[19].

REGN5381 in normotensive monkeys

We next extended the above observations, that is, that REGN5381 can mimic native NP-like haemodynamic actions to primates, by examining normotensive male cynomolgus monkeys. A single subcutaneous 1, 5 or 25 mg per kg or intravenous 5 or 25 mg per kg dose of REGN5381 persistently reduced systolic BP by 10–15 mm Hg for up to 55 days (end of study) in the 25 mg per kg groups (Fig. 4e and Supplementary Fig. 5). In agreement with that, the exposure of REGN5381 in serum after the 25 mg per kg intravenous or subcutaneous dose was sustained throughout the study duration (Extended Data Fig. 7). As also seen in normotensive mice and canines, this reduction was associated with the expected compensatory increase in heart rate (Fig. 4f). Native NPs induce decreases in stroke volume and cardiac output in healthy humans (although, consistent with Frank–Starling, they improve both in patients with HF), which is reflected by a reduction in pulse pressure. Consistent with this, we saw a dose-dependent reduction in pulse pressures in this monkey study (Fig. 4g). Moreover, as also seen in the other species, a REGN5381-related increase in urinary cGMP and a decrease in NT-proANP was observed for all dose groups (Fig. 4h and Extended Data Fig. 8).

REGN5381 in healthy adults

The above data in mice, canines and monkeys indicated that REGN5381 was acting like a durable mimetic of NPs. To extend these observations to humans, a total of 48 healthy adults were randomized to receive a single intravenous injection of REGN5381 (0.3, 1, 3, 10, 30 or 100 mg) or placebo: 6 adults per active dose group and 12 adults were treated with placebo. The highest REGN5381 dose (100 mg) was associated with a 6–9 mm Hg reduction in systolic BP, seen throughout the 72 h observation period (Fig. 5a). As expected, and as seen in the preclinical species, this reduction in systolic BP was associated with a modest increase in heart rate (Fig. 5b). Also consistent with the previous REGN5381 data in preclinical species, and as seen with native NPs in healthy adults, REGN5381 also resulted in a narrowing of pulse pressures and reduction in stroke volume (Fig. 5c,d). These haemodynamic changes were associated with a sustained increase in urine cGMP (Fig. 5e). Notably, as also seen in the preclinical species, there was no change in urine output across all dose cohorts (Fig. 5f). REGN5381 also induced plasma cGMP production in healthy volunteers (Extended Data Fig. 9).

A single intravenous dose of REGN5381 was generally well tolerated. Moreover, no serious treatment-emergent adverse events (TEAEs), severe TEAEs or deaths were reported throughout the study period. In an unblinded safety analysis, treatment-related TEAEs were reported in 15 (42%) adults receiving REGN5381 and 4 (33%) adults receiving placebo. The most frequent TEAE was postural dizziness ($n = 6$ receiving REGN5381, $n = 2$ receiving placebo) and did not have any obvious relationship to the dose level. Additional treatment-related TEAEs occurring in more than 10% of adults included feeling hot and orthostatic hypotension (Table 1). Across all dose cohorts, no clinically important or dose-dependent treatment-emergent changes in haematological and chemistry parameters were observed through the end-of-study visit (up to 77 days after study drug administration). Two participants in the lower-dose cohorts (0.3 and 3 mg) were found to have self-limited, non-sustained ventricular tachycardia (four beats)

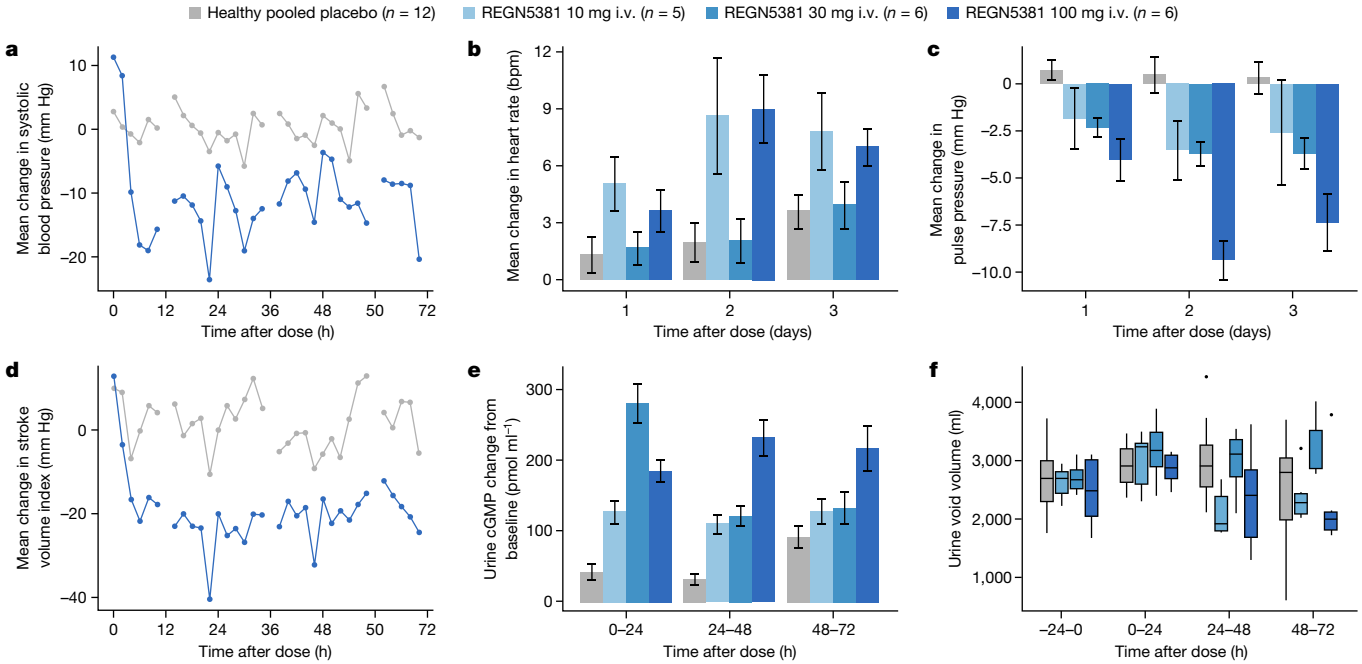

Fig. 5 | REGN5381 reduces systolic BP and stroke volume, and increases pulse rate, in healthy volunteers. a, The effect of intravenous REGN5381 100 mg ($n = 6$, blue line) or placebo ($n = 12$, grey line) on systolic BP, as measured by pulse-wave analysis (PWA), presented as the time-matched change from baseline. Pressure is presented as the average over 2 h. **b**, The time-matched mean change from baseline in heart rate, assessed by pulse-wave analysis, according to intravenous treatment group (pooled placebo, grey bar; REGN5381 10 mg, light blue bar; REGN5381 30 mg, blue bar; REGN5381 100 mg, dark blue bar). The mean change from baseline in heart rate and pulse pressure is shown as the average over 24 h. **c**, The time-matched mean change from baseline in pulse pressure assessed by pulse-wave analysis according to intravenous treatment group (pooled placebo, grey bar; REGN5381, 10 mg, light blue bar; REGN5381, 30 mg, blue bar; REGN5381, 100 mg, dark blue bar). **d**, The effect of intravenous REGN5381 100 mg ($n = 6$, blue line) or placebo ($n = 12$, grey line) on the stroke volume index as measured by pulse-wave analysis, shown as the time-matched change from baseline. The stroke volume index is shown as the average over 2 h. **e**, The change from baseline in urine cGMP levels after administration of study treatment (pooled placebo, grey bar; REGN5381, 10 mg, light blue bar; REGN5381, 30 mg, blue bar; REGN5381, 100 mg, dark blue bar). Data are mean ± s.e.m. **f**, The urine void volume was assessed before and after dosing according to treatment group (pooled placebo, grey bar; REGN5381, 10 mg, light blue bar; REGN5381, 30 mg, blue bar; REGN5381, 100 mg, dark blue bar).

that was identified on telemetry as part of the 96 h monitoring period, per protocol. Arrhythmias occurred in fewer than 10% of participants receiving REGN5381 or placebo and did not require intervention. No other clinically important abnormalities or dose-dependent shifts from baseline in vital signs or in any electrocardiogram (ECG) parameters were observed across all cohorts until the end-of-study visit. All of the participants met in-patient discharge criteria at 72 h.

Discussion

Here we describe an investigational agonist monoclonal antibody, REGN5381, that targets and activates NPR1. We demonstrate that this agonist antibody mirrors the haemodynamic and pharmacodynamic effects of native NPs (in mice, canines, monkeys and humans), potentially providing a convenient and long-acting therapeutic that can achieve and extend the demonstrated benefits of continuous NP infusion in patients with HF. Thus far, the infusion approach has limited applications to the in-hospital setting.

Moreover, we provide human genetic analyses confirming and extending previous claims that genetic LOF variants in the NPR1 receptor result in increased BP, higher NT-proBNP and increased HF risk, while genetic GOF variants result in decreased BP, lower levels of NT-proBNP and presumably lower risk of HF. These findings are consistent with the known biology of NPs, and their associated increased release from the heart in response to increased pressure, and support the therapeutic rationale for long-acting therapeutics activating NPR1.

It has been shown that native NPs reduce preload and PCWP. In normal healthy adults, this results in reduced venous filling during the cardiac cycle, lower stroke volumes, and reduced cardiac output; we have shown similar effects of REGN5381 in four different species, from mice to humans. By contrast, it is well known that patients with congested HF have elevated venous pressures, including PCWP, which results in many of the signs and symptoms of HF. The elevated PCWP leads to pulmonary oedema and congestion, causing inadequate oxygenation and dyspnoea; thus, one goal in HF is to reduce pulmonary oedema and congestion, which should be achieved by lowering PCWP. Furthermore, elevated preload results in over-filling of the heart, dilation, and decreases in stroke volume and cardiac output. Owing to the position of patients with HF on the Frank–Starling curve, it is hypothesized that decreasing preload in these patients would increase the stroke volume and cardiac output, in contrast to what is seen when preload is lowered in healthy adults.

On the basis of the above, the ability of native NPs to decrease preload in HF could benefit patients by both decreasing pulmonary congestion (and therefore improving oxygenation) and also by reducing excess filling of the heart and therefore improving stroke volume and cardiac output. Indeed, stroke volume was shown to improve when patients with congestive HF received treatment with continuous infusions of recombinant ANP and BNP[19,27], and infusion of ANP is approved for acute HF in Japan. As REGN5381 largely mirrors the haemodynamic effects of infused native NPs, it may provide for a convenient and durable way to benefit patients with HF by reducing preload and PCWP, thereby improving both pulmonary oedema and possibly also improving cardiac output. Moreover, if proven safe and well-tolerated, it may allow these benefits in the chronic, out-patient setting.

Table 1 | Treatment-related adverse events by treatment assignment

	REGN5381, i.v.							
	Placebo, i.v. total	0.3 mg	1 mg	3 mg	10 mg	30 mg	100 mg	Total
Primary SOC PT	***n*=12**	***n*=6**	***n*=6**	***n*=6**	***n*=6**	***n*=6**	***n*=6**	***n*=36**
Number of treatment-related TEAEs	11	4	1	3	4	8	6	26
Participants with at least one treatment-related TEAE, *n* (%)	4 (33.3)	3 (50.0)	1 (16.7)	2 (33.3)	3 (50.0)	3 (50.0)	3 (50.0)	15 (41.7)
Nervous system disorders, *n* (%)	4 (33.3)	2 (33.3)	0	0	1 (16.7)	3 (50.0)	2 (33.3)	8 (22.2)
Dizziness postural	2 (16.7)	1 (16.7)	0	0	1 (16.7)	3 (50.0)	1 (16.7)	6 (16.7)
Dizziness	1 (8.3)	0	0	0	0	0	1 (16.7)	1 (2.8)
Headache	1 (8.3)	1 (16.7)	0	0	0	0	0	1 (2.8)
Presyncope	0	0	0	0	0	0	1 (16.7)	1 (2.8)
Cardiac disorders, *n* (%)	1 (8.3)	1 (16.7)	1 (16.7)	1 (16.7)	1 (16.7)	0	1 (16.7)	5 (13.9)
Palpitations	1 (8.3)	0	1 (16.7)	0	1 (16.7)	0	1 (16.7)	3 (8.3)
Ventricular tachycardia	0	1 (16.7)	0	1 (16.7)	0	0	0	2 (5.6)
Vascular disorders, *n* (%)	0	1 (16.7)	0	0	1 (16.7)	2 (33.3)	1 (16.7)	5 (13.9)
Orthostatic hypotension	0	0	0	0	1 (16.7)	2 (33.3%)	1 (16.7)	4 (11.1)
Diastolic hypotension	0	1 (16.7)	0	0	0	0	0	1 (2.8)
Gastrointestinal disorders, *n* (%)	1 (8.3)	0	0	1 (16.7)	0	2 (33.3)	1 (16.7)	4 (11.1)
Nausea	0	0	0	0	0	2 (33.3)	1 (16.7)	3 (8.3)
Diarrhoea	1 (8.3)	0	0	1 (16.7)	0	0	0	1 (2.8)
Vomiting	0	0	0	1 (16.7)	0	0	0	1 (2.8)
General disorders and administration site conditions, *n* (%)	2 (16.7)	0	0	0	1 (16.7)	1 (16.7)	0	2 (5.6)
Feeling hot	2 (16.7)	0	0	0	1 (16.7)	1 (16.7)	0	2 (5.6)

The Medical Dictionary for Regulatory Activities (MedDRA) (v.25.1) coding dictionary was applied. At each level of participant summarization, a participant is counted once if the participant reported one or more events. i.v., intravenous; SOC, system organ class; PT, preferred term.

Our in vivo studies suggest that REGN5381 has a floor in its ability to lower systolic BP. In vivo, supraphysiological levels of the endogenous NPR1 ligands ANP and BNP induced an approximately 30 mm Hg sustained reduction in systolic BP in normotensive mice compared with a maximal 10–15 mm Hg reduction with REGN5381. Consistent with the possibility that REGN5381 is a partial agonist, REGN5381 led to a maximum activation of NPR1 in vitro that was lower than that achieved by native ligands in the cGMP accumulation assay (Extended Data Fig. 3). Our structural biology studies on REGN5381 suggest an allosteric activation mechanism that may explain the above observations. REGN5381 can bind to an NPR1 dimer (one Fab arm per NPR1 monomer, as shown in Fig. 2), producing a conformation that is similar to the active state of NPR1, even in the absence of a bound peptide. The bound Fabs stabilize this active-like state: it is not possible for the monomers to rotate back to the parallel, inactive state seen with ANP-free NPR1 (Fig. 2a), as this rotation would cause a steric clash between the two bound Fabs (Supplementary Fig. 6). Returning the NPR1 dimer to its inactive state requires the dissociation of one or both REGN5381 Fabs, which is energetically unfavourable. Our data suggest that this active-like state can lead to downstream signalling, as shown in the NPR1 bioassay with REGN5381 Fab (Supplementary Fig. 7). However, REGN5381-activated NPR1 may not be fully active, possibly because the conformation is not exactly the same as ANP-activated NPR1 or the affinity towards NPR1 needs to be more potent (Fig. 2). Taken together, in vivo studies, in vitro activation studies and structural biology assessment provide insights into a potential mechanism for the observed floor in pressure seen in preclinical studies incorporating high doses of REGN5381. These findings indicate that REGN5381 may have a unique safety attribute whereby the potential of undesirable pharmacology could be limited, regardless of dose.

Sacubitril/valsartan is approved for patients with HF and is a combination of a neprilysin inhibitor and an angiotensin receptor blocker. The sacubitril component of sacubitril/valsartan inhibits neprilysin-mediated degradation of ANP or BNP, increasing NP levels. However, as neprilysin degrades multiple substrates, including bradykinin and angiotensin II[28], inhibition of neprilysin increases angiotensin II levels, thereby increasing renin–angiotensin–aldosterone system activation and elevating systolic BP. Administration of neprilysin inhibitors has been linked to increased rates of angioedema, possibly due to bradykinin accumulation[29]. Concurrent administration with an angiotensin receptor blocker negates renin–angiotensin–aldosterone-system-related undesired effects, but also reduces systolic BP. REGN5381 offers a specific approach for agonizing NPR1 that may allow greater NPR1 activation and, therefore, greater preload reduction, while eliminating the untoward issues associated with the non-specific inhibition of neprilysin. Furthermore, the long duration of effect of REGN5381 provides a more durable method of NPR1 agonism than is achieved by neprilysin inhibition.

The absence of an observed diuretic response in three separate preclinical species (Supplementary Figs. 8 and 9) and a first-in-human trial was surprising and largely contrary to the central dogma of NPs. However, these findings are consistent with a previously published lack of effect on urine output after recombinant BNP infusion[30]. Furthermore, the multifactorial changes that occur after NPR1 agonism suggest that perhaps multiple downstream signalling pathways are involved in the regulation of global haemodynamics and these pathways are dependent on the current haemodynamic environment[31]. One limitation of the current body of work is the lack of evaluation of REGN5381 in the presence of volume expansion or congestion. We hypothesize that NPR1-mediated diuresis may occur only under a fluid-loaded state, for which no preclinical models were evaluated.

Other limitations include the lack of a preclinical model of venous congestion and the small sample size in the first-in-human trial. Further trials are needed to extend the results from healthy adults to those with HF.

In conclusion, REGN5381 is an investigational and novel fully human antibody that is an agonist of a guanylate cyclase receptor that elicits an active-like conformation of NPR1. Our preclinical and first-in-human results in healthy adults indicate that REGN5381 provides sustained haemodynamic effects, with no evidence of adverse hypotension. Overall, the results suggest that REGN5381 could offer a long-acting therapeutic that could benefit patients by specifically reducing CVP, which is abnormally increased in patients with HF; the ability to reduce elevated CVP, without causing adverse hypotension, could provide therapeutically important improvements in pulmonary oedema and cardiac output for these patients. Benefits may also be provided in cardiovascular and renal conditions in which elevated venous pressures occur. Further research is needed to assess the safety and efficacy of REGN5381 in patients with HF.

Online content

Any methods, additional references, Nature Portfolio reporting summaries, source data, extended data, supplementary information, acknowledgements, peer review information; details of author contributions and competing interests; and statements of data and code availability are available at https://doi.org/10.1038/s41586-024-07903-1.

1. Lippi, G. & Sanchis-Gomar, F. Global epidemiology and future trends of heart failure. *AME Med. J.* **5**, 15 (2020).
2. Bowen, R. E. S., Graetz, T. J., Emmert, D. A. & Avidan, M. S. Statistics of heart failure and mechanical circulatory support in 2020. *Ann. Transl. Med.* **8**, 827 (2020).
3. Ledsome, J. R., Wilson, N., Courneya, C. A. & Rankin, A. J. Release of atrial natriuretic peptide by atrial distension. *Can. J. Physiol. Pharmacol.* **63**, 739–742 (1985).
4. Levin, E. R., Gardner, D. G. & Samson, W. K. Natriuretic peptides. *N. Engl. J. Med.* **339**, 321–328 (1998).
5. Ramos, H. & de Bold, A. J. Gene expression, processing, and secretion of natriuretic peptides: physiologic and diagnostic implications. *Heart Fail. Clin.* **2**, 255–268 (2006).
6. Ogawa, T. & de Bold, A. J. The heart as an endocrine organ. *Endocr. Connect.* **3**, R31–R44 (2014).
7. Toyoshima, Y. et al. Atrial natriuretic peptide (ANP)-granules of auricular cardiocytes in dehydrated and rehydrated mice. *Exp. Anim.* **45**, 135–140 (1996).
8. DeBold, A. J., Borenstein, H. B., Verres, A. T. & Sonnenberg, H. A rapid and potent natriuretic response to intravenous injection of atrial extracts in rats. *Life Sci.* **28**, 89–94 (1981).
9. Katz, S. D. Nesiritide (hbNP): a new class of therapeutic peptide for the treatment of decompensated congestive heart failure. *Congest. Heart Fail.* **7**, 78–87 (2007).
10. Fu, S., Ping, P., Wang, F. & Luo, L. Synthesis, secretion, function, metabolism and application of natriuretic peptides in heart failure. *J. Biol. Eng.* **12**, 2 (2018).
11. Cautela, J. et al. Management of low blood pressure in ambulatory heart failure with reduced ejection fraction patients. *Eur. J. Heart Fail.* **22**, 1357–1365 (2020).
12. Gidlof, O. Toward a new paradigm for targeted natriuretic peptide enhancement in heart failure. *Front. Physiol.* **12**, 650124 (2021).
13. Kuhn, K. P. et al. Outcome in 91 consecutive patients with pulmonary arterial hypertension receiving epoprostenol. *Am. J. Respir. Crit. Care Med.* **167**, 580–586 (2003).
14. Schmitt, M. et al. Atrial natriuretic peptide regulates regional vascular volume and venous tone in humans. *Arterioscler. Thromb. Vasc. Biol.* **23**, 1833–1838 (2003).
15. Vandenwijngaert, S. et al. Blood pressure-associated genetic variants in the natriuretic peptide receptor 1 gene modulate guanylate cyclase activity. *Circ. Genom. Precis. Med.* **12**, e002472 (2019).
16. Liu, C. et al. Meta-analysis identifies common and rare variants influencing blood pressure and overlapping with metabolic trait loci. *Nat. Genet.* **48**, 1162–1170 (2016).
17. Surendran, P. et al. Discovery of rare variants associated with blood pressure regulation through meta-analysis of 1.3 million individuals. *Nat. Genet.* **52**, 1314–1332 (2020).
18. Novartis Pharmaceuticals. Entresto prescribing information. *Novartis* https://www.novartis.com/us-en/sites/novartis_us/files/entresto.pdf (April 2024).
19. Saito, Y. et al. Clinical application of atrial natriuretic polypeptide in patients with congestive heart failure: beneficial effects on left ventricular function. *Circulation* **76**, 115–124 (1987).
20. Lakatta, E. in *The Heart and Cardiovascular System* (ed. Fozzard, H.A.) 1325–1351 (Raven Press, 1992).
21. Macdonald, L. E. et al. Precise and in situ genetic humanization of 6 Mb of mouse immunoglobulin genes. *Proc. Natl Acad. Sci. USA* **111**, 5147–5152 (2014).
22. Murphy, A. J. et al. Mice with megabase humanization of their immunoglobulin genes generate antibodies as efficiently as normal mice. *Proc. Natl Acad. Sci. USA* **111**, 5153–5158 (2014).
23. Wunder, F. et al. A cell-based cGMP assay useful for ultra-high-throughput screening and identification of modulators of the nitric oxide/cGMP pathway. *Anal. Biochem.* **339**, 104–112 (2005).
24. Ogawa, H., Qiu, Y., Ogata, C. M. & Misono, K. S. Crystal structure of hormone-bound atrial natriuretic peptide receptor extracellular domain: rotation mechanism for transmembrane signal transduction. *J. Biol. Chem.* **279**, 28625–28631 (2004).
25. van den Akker, F. et al. Structure of the dimerized hormone-binding domain of a guanylyl-cyclase-coupled receptor. *Nature* **406**, 101–104 (2000).
26. Thomas, C. J. & Woods, R. L. Haemodynamic action of B-type natriuretic peptide substantially outlasts its plasma half-life in conscious dogs. *Clin. Exp. Pharmacol. Physiol.* **30**, 369–375 (2003).
27. Hobbs, R. E. et al. Hemodynamic effects of a single intravenous injection of synthetic human brain natriuretic peptide in patients with heart failure secondary to ischemic or idiopathic dilated cardiomyopathy. *Am. J. Cardiol.* **78**, 896–901 (1996).
28. Potter, L. R. Natriuretic peptide metabolism, clearance and degradation. *FEBS J.* **278**, 1808–1817 (2011).
29. Kostis, J. B. et al. Omapatrilat and enalapril in patients with hypertension: the omapatrilat cardiovascular treatment vs. enalapril (OCTAVE) trial. *Am. J. Hypertens.* **17**, 103–111 (2004).
30. Gottlieb, S. S. et al. Effects of nesiritide and predictors of urine output in acute decompensated heart failure: results from ASCEND-HF (acute study of clinical effectiveness of nesiritide and decompensated heart failure). *J. Am. Coll. Cardiol.* **62**, 1177–1183 (2013).
31. Wagner, B. M. et al. Guanylyl cyclase-A phosphorylation decreases cardiac hypertrophy and improves systolic function in male, but not female, mice. *FASEB J.* **36**, e22069 (2022).

Penn Medicine Biobank

Daniel J. Rader[8], Marylyn D. Ritchie[8], JoEllen Weaver[8], Nawar Naseer[8], Afiya Poindexter[8], Khadijah Hu-Sain[8], Yi-An Ko[8], Meghan Livingstone[8], Fred Vadivieso[8], Stephanie DerOhannessian[8], Teo Tran[8], Julia Stephanowski[8], Monica Zielinski[8], Ned Haubein[8], Joseph Dunn[8], Anurag Verma[8], Colleen Morse Kripke[8], Marjorie Risman[8], Renae Judy[8], Shefali S. Verma[8], Yuki Bradford[8], Scott Dudek[8] & Theodore Drivas[8]

GHS-RGC DiscovEHR Collaboration

Lance J. Adams[9], Jackie Blank[9], Dale Bodian[9], Derek Boris[9], Adam Buchanan[9], David J. Carey[9], Ryan D. Colonie[9], F. Daniel Davis[9], Dustin N. Hartzel[9], Melissa Kelly[9], H. Lester Kirchner[9], Joseph B. Leader[9], David H. Ledbetter[9], J. Neil Manus[9], Christa L. Martin[9], Raghu P. Metpally[9], Michelle Meyer[9], Tooraj Mirshahi[9], Matthew Oetjens[9], Thomas Nate Person[9], Christopher Still[9], Natasha Strande[9], Amy Sturm[9], Jen Wagner[9] & Marc Williams[9]

Regeneron Genetics Center

Goncalo Abecasis[3], Aris Baras[3], Michael Cantor[3], Giovanni Coppola[3], Andrew Deubler[3], Aris Economides[3], Luca A. Lotta[3], John D. Overton[3], Jeffrey G. Reid[3], Katherine Siminovitch[3], Alan Shuldiner[3], Christina Beechert[3], Caitlin Forsythe[3], Erin D. Fuller[3], Zhenhua Gu[3], Michael Lattari[3], Alexander Lopez[3], Maria Sotiropoulos Padilla[3], Manasi Pradhan[3], Kia Manoochehri[3], Thomas D. Schleicher[3], Louis Widom[3], Sarah E. Wolf[3], Ricardo H. Ulloa[3], Amelia Averitt[3], Nilanjana Banerjee[3], Michael Cantor[3], Dadong Li[3], Sameer Malhotra[3], Deepika Sharma[3], Jeffrey C. Staples[3], Xiaodong Bai[3], Suganthi Balasubramanian[3], Suying Bao[3], Boris Boutkov[3], Siying Chen[3], Gisu Eom[3], Lukas Habegger[3], Alicia Hawes[3], Shareef Khalid[3], Olga Krasheninina[3], Rouel Lanche[3], Adam J. Mansfield[3], Evan K. Maxwell[3], George Mitra[3], Mona Nafde[3], Sean O'Keeffe[3], Max Orelus[3], Razvan Panea[3], Tommy Polanco[3], Ayesha Rasool[3], William Salerno[3], Kathie Sun[3], Joshua Backman[3], Amy Damask[3], Lee Dobbyn[3], Manuel Allen Revez Ferreira[3], Arkopravo Ghosh[3], Christopher Gillies[3], Lauren Gurski[3], Eric Jorgenson[3], Hyun Min Kang[3], Michael Kessler[3], Jack Kosmicki[3], Alexander Li[3], Nan Lin[3], Daren Liu[3], Adam Locke[3], Jonathan Marchini[3], Anthony Marcketta[3], Joelle Mbatchou[3], Arden Moscati[3], Charles Paulding[3], Carlo Sidore[3], Eli Stahl[3], Kyoko Watanabe[3], Bin Ye[3], Blair Zhang[3], Andrey Ziyatdinov[3], Ariane Ayer[3], Aysegul Guvenek[3], George Hindy[3], Giovanni Coppola[3], Jan Freudenberg[3], Jonas Bovijn[3], Kavita Praveen[3], Manav Kapoor[3], Mary Haas[3], Moeen Riaz[3], Niek Verweij[3], Olukayode Sosina[3], Parsa Akbari[3], Priyanka Nakka[3], Sahar Gelfman[3], Sujit Gokhale[3], Tanima De[3], Veera Rajagopal[3], Gannie Tzoneva[3], Juan Rodriguez-Flores[3], Esteban Chen[3], Marcus B. Jones[3], Michelle G. LeBlanc[3], Jason Mighty[3], Lyndon J. Mitnaul[3], Nirupama Nishtala[3], Nadia Rana[3], Jaimee Hernandez[3] & Jennifer Rico Varela[3]

[8]Department of Medicine, Perelman School of Medicine, University of Pennsylvania, Philadelphia, PA, USA. [9]Geisinger, Danville, PA, USA.

Methods

Human genetics assessment

Population cohorts. We included 453,072 participants in the UK Biobank, 164,353 participants in Geisinger Health System MyCode cohort, 41,251 participants in the Penn Medicine Biobank (UPENN-PMBB), 28,935 participants in the Malmö Diet and Cancer Study, 26,035 participants in the Mount Sinai BioMe Biobank and 4,736 participants recruited from Indiana University School of Medicine[32,33]. Systolic and diastolic BP readings were obtained from participants in the UK Biobank, Geisinger Health System MyCode cohort, UPENN-PMBB and the Malmö Diet and Cancer Study. In case of more than one BP reading, we used the median value. To correct for treatment with anti-hypertensive medication, 15 mm Hg was added to systolic BP readings and 10 mm Hg to diastolic BP readings in individuals with a history of treatment with anti-hypertensive medication, as previously done[34,35]. NT-proBNP was measured in the UK Biobank using a proteomics assay Olink[36]; in the Geisinger Health System MyCode cohort, measurements were extracted from electronic health records. HF was defined on the basis of International Classification of Diseases codes and procedure codes obtained from electronic health records as summarized in Supplementary Table 6.

DNA sequencing and genotyping data. The Regeneron Genetics Center performed high-coverage whole-exome sequencing using NimbleGen VCRome probes (Roche) or a modified version of the xGen design from Integrated DNA Technologies (IDT). Sequencing was performed using the Illumina v4 HiSeq 2500 or NovaSeq instrument, achieving over 20× coverage for 96% of VCRome samples and 99% of IDT samples. Variants were annotated using snpEff and Ensembl v85 gene definitions, prioritizing protein-coding transcripts on the basis of functional impact. The following variants were defined as protein truncating: insertions or deletions resulting in frameshift, any variant causing a stop gained, start lost or stop lost and any variants affecting a splice acceptor or splice donor site. Common-variant genotyping was performed on one of three single-nucleotide polymorphism array types as previously described: Illumina OmniExpress Exome array, Applied Biosystems UK BiLEVE Axiom Array or Applied Biosystems UK Biobank Axiom Array. We retained genotyped variants with a minor allele frequency (MAF) of >1%, <10% missingness and Hardy–Weinberg equilibrium test $P > 10^{-15}$. We imputed the genotyped variants using the TOPMed reference panel[37] using the TOPMed imputation server[38,39]. In GHS, imputation was performed separately by genotyping platform. Further details are provided elsewhere[32,33,40,41].

Association analyses. We estimated associations between protein-altering variants in NPR1 and phenotypes by fitting additive genetic, linear regression models (for quantitative traits; BP and NT-proBNP) or Firth bias-corrected logistic regression models (for binary traits; HF) using REGENIE (v.2+) software[42]. Analyses were stratified according to ancestry and were adjusted for age, age squared, sex, age-by-sex and age squared-by-sex interaction terms; experimental batch-related covariates; the first 10 common-variant–derived genetic principal components; the first 20 rare-variant-derived principal components; and a polygenic score generated by REGENIE, which robustly adjusts for relatedness and population structure[42]. Association results were meta-analysed across cohorts and ancestries using fixed-effects inverse variance weighting.

In addition to analysing individual protein-altering variants in *NPR1*, we evaluated two sets of gene-based burden genotypes: (1) a collection of rare predicted LOF variants; and (2) collections that include rare missense variants that are predicted to be GOF or LOF on the basis of experimental evidence or their association with BP. To characterize GOF or LOF, we first tested for association of rare and low-frequency (MAF < 1%), protein-truncating variants (presumed LOF) in *NPR1* with BP and NT-proBNP across all available samples. Second, after exclusion of individuals with HF, we randomly split the cohorts with available BP readings in half into training sets (half of the samples) and test sets (half of the samples). All protein-altering variants in *NPR1* with MAF < 1% and a minor allele count of ≥10 associated with increased systolic or diastolic BP ($P < 0.05$) in the training set were characterized as presumed LOF, whereas variants associated with decreased systolic or diastolic BP in the training set were characterized as presumed GOF. The three previously published LOF or GOF variants[15] were included regardless of these variant selection criteria. We then tested for association of the burden of presumed GOF and LOF variants with BP in the test sets and with NT-proBNP and HF in the combined set of test set samples and HF samples.

Generation of REGN5381

Fully human monoclonal antibodies against NPR1 were generated using VelocImmune technology[21,22]. The VelocImmune platform uses mice that are genetically modified to produce antibodies with human variable regions and enables efficient selection and development of fully human antibodies. Mice were immunized by the co-injections of human NPR1 and mouse ANP-expressing DNA plasmids, boosted with a protein complex of ANP–hNPR1. From the high-titre mice, splenocytes were isolated, and clones producing antibodies with desirable properties were identified and cloned to produce recombinant antibody proteins.

Surface plasmon resonance binding

The kinetics of REGN5381 NPR1-specific monoclonal antibody binding to NPR1 proteins were determined on the Biacore 8K, Biacore 4000, T200 or S200 biosensor (Cytiva), using the Series S CM4 sensor chip in filtered and degassed HEPES-buffered saline running buffer (10 mM HEPES, 150 mM NaCl, 3 mM EDTA, 0.05% (v/v) polysorbate 20, pH 7.4) at 25 °C or 37 °C. The CM4 sensor chip was immobilized with mouse anti-human fragment crystallizable region (Fc) monoclonal antibody (REGN2567) or mouse anti-His monoclonal antibody (Cytiva) using standard amine-coupling chemistry[43]. REGN5381 NPR1 monoclonal antibodies were captured (100 RU-685 RU) through their Fc regions on anti-human Fc immobilized surfaces and varying concentrations of extracellular domains of NPR1, NPR2 and NPR3 proteins (with C-terminal MycMycHis) and ANP were injected followed by a dissociation phase. At the end of each cycle, anti-human-Fc-captured NPR1-specific monoclonal antibodies were removed using a 12 s injection of 20 mmol l^{-1} phosphoric acid.

All of the specific surface plasmon resonance-binding sensorgrams were double-reference-subtracted as reported previously[44], and the kinetic parameters were obtained by globally fitting the double-reference-subtracted data to a 1:1 binding model with mass transport limitation using Biacore Insight Evaluation software (Cytiva). The dissociation rate constant (k_d) was determined by fitting the change in the binding response during the dissociation phase, and the association rate constant (k_a) was determined by globally fitting analyte binding at different concentrations. The equilibrium dissociation constant (K_D) was calculated from the ratio of k_d and k_a. The dissociative half-life in minutes was calculated as $\ln 2/(k_d \times 60)$.

Cell binding and NPR1 bioassays

HEK293 cell lines were generated to stably express hNPR1 (amino acids M1 to G1061 of NP_000897.3) with C-terminal MYC and Flag tags or mfNPR1 (amino acids M1 to G1061 of XP_005541809.1). Flow cytometry experiments were performed with antibodies with or without 100 nM of human ANP or BNP (CytoFLEX flow cytometer) and the results were analysed using FlowJo. To assess NPR1 activity, bovine CNGA2 (amino acids Met1 to Pro663 of UniProt Q03041) was expressed along with NPR1. CNGA2 is a cation channel that can be activated by cGMP and can therefore be used as a readout for cGMP production[23]. NPR1 activation was monitored by measuring calcium influx through CNGA2 using a fluorescent Ca^{2+} indicator (Invitrogen Fluo-4 Direct Calcium Assay

Kit; FLIPR TETRA, Molecular Devices). The numeric Ca^{2+} flux signal (one read per s, 700 total), expressed in relative fluorescence units, was calculated as the area under the time-signal-intensity curve from which the background signal observed before the addition of test reagents was subtracted. NPR1 activity was also evaluated by cGMP production (Cisbio cGMP kit, 62GM2PEH) with REGN5381 in the absence or presence of ligand at either 37 °C with 20,000 cells or room temperature with 1,000 cells. HEK293 cells have been authenticated via Human 16-Marker STR profile (IDEXX BioAnalytics) to be >80% identical to HEK293 cells sourced from ATCC, and tested negative for mycoplasma.

Physical complex assessment

A4F-MALS was used to assess the relative size distribution of complexes formed between REGN5381, hNPR1 ectodomain (REGN3037) and ANP. The A4F-MALS system is composed of a Wyatt Eclipse instrument and channel coupled to an Agilent 1260 Series High Performance Liquid Chromatography system equipped with an ultraviolet (UV) diode array detector, Wyatt Technology DAWN laser light-scattering (LS) instrument and an Optilab T-rEX differential refractometer (RI) detector. The detectors were connected in series in the following order: UV–LS–RI. The detector flow was maintained at 1.0 ml min^{-1} for the duration of the run, and the samples were injected onto the channel at 0.2 ml min^{-1} and were focused for 3 min using a focus flow rate of 1.5 ml min^{-1}. The separation step consisted of a linear gradient of the crossflow from 2.0 ml min^{-1} to 0.0 ml min^{-1} over 45 min before holding the crossflow for a further 5 min at 0.0 ml min^{-1} to allow any large particles to elute. The spacer in the channel was 350 W (Wyatt, 350 Å in height) while the membrane was 10 kDa MWCO regenerated cellulose (Wyatt). The mobile phase for all experiments was 10 mM sodium phosphate and 500 mM NaCl pH 7.0 ± 0.1.

Cryo-EM analysis

Sample preparation and data collection. The NPR1 soluble domain was mixed with molar excess of the Fab fragment of REGN5381 in the presence or absence of ANP. The complex was incubated overnight at 4 °C then purified over the Superdex 200 increase 10/300 GL gel-filtration column equilibrated with 50 mM Tris pH 7.5 and 150 mM NaCl. Peak fractions containing the NPR1-REGN5381 Fab complex were collected and concentrated using a 10 kDa molecular weight cut-off centrifugal concentrator (Amicon). For cryo-EM grid preparation, the protein sample was diluted to 1.6 mg ml^{-1} and 0.15% poly(maleic anhydride-alt-1-decene)-C8 amphipol was added. Then, 3 µl of protein was deposited onto a freshly plasma cleaned UltrAufoil grid (0.6/1, 300 mesh) using the Gatan Solarus II (Gatan) system. Excess solution was blotted away using filter paper and plunge-frozen into liquid ethane using the Vitrobot Mark IV (Thermo Fisher Scientific). The cryo-EM grid was transferred to a Titan Krios (Thermo Fisher Scientific) operated at 300 kV and equipped with a K3 detector (Gatan). Automated data collection was carried out using EPU (Thermo Fisher Scientific) at a nominal magnification of ×105,000, corresponding to a pixel size of 0.86 Å. A dose rate of 15 e− px^{-1} s^{-1} was used and each video was 2 s, corresponding to a total dose of around 40 e^{-} $Å^{-2}$. The defocus ranged from −1.4 to −2.4 µm.

NPR1–REGN5381 Fab–ANP complex. All cryo-EM data processing was performed using cryoSPARC (v.3.2.0)[45]. A total of 6,717 videos were collected; after alignment using patch motion correction followed by patch contrast transfer function estimation, 6,313 videos were selected for particle picking. An initial set of particles picked using a blob picker were subjected to 2D classification to generate templates for template picking (Extended Data Fig. 4a–c). In total, around 1.16 million particles picked by template picking were subjected to multiple rounds of 2D classification, yielding around 1.04 million particles in the optimal classes. Ab initio reconstruction with six classes generated different states of the NPR1 dimer with the REGN5381 Fab; the highest-resolution class had 682,951 particles corresponding to an NPR1 dimer with two REGN5381 Fabs and ANP bound. Non-uniform refinement of the particles in this class, followed by local refinement, resulted in a 3.1-Å-resolution (Fourier shell correlation = 0.143) map that was used for model building. Into this map, we manually placed models of NPR1 dimer in complex with ANP (PDB: 1T34) and two Fabs (derived from other Regeneron antibody structures). These models were then manually rebuilt using Coot[46], and real-space refined against the map using Phenix[47]. Cryo-EM data and model statistics are provided in Extended Data Table 1.

NPR1–REGN5381 Fab complex (no ANP). For this complex, a total of 6,541 videos were collected; after alignment using patch motion correction followed by patch contrast transfer function estimation, 6,324 videos were selected for particle picking. An initial set of particles picked using a blob picker were subjected to 2D classification to generate templates for template picking (Extended Data Fig. 4d–f). In total, around 1.3 million particles picked by template picking were subjected to multiple rounds of 2D classification, yielding about 0.96 million particles in the optimal classes. Ab initio reconstruction with three classes generated different states of the NPR1 dimer with the REGN5381 Fab; the highest resolution class had 495,382 particles corresponding to an NPR1 dimer with two REGN5381 Fabs and ANP bound. Non-uniform refinement of the particles in this class, followed by local refinement, resulted in a 3.65-Å-resolution (Fourier shell correlation = 0.143) map. This dataset has substantial preferred particle orientation, and the map resolution is anisotropic and, in many areas, a good deal worse than 3.65 Å (Extended Data Fig. 4d). Although this map clearly defined the overall conformation of the NPR1–REGN5381 complex, and showed no density at the ANP-binding site (Extended Data Fig. 4d), it was not feasible to carry out model building and refinement in the manner that we did for the NPR1–REGN5381–ANP complex. Instead, that complex model was split into two half-complex models, each containing one NPR1 ectodomain and one REGN5381 Fab. These half-complexes were rigid-body refined against the NPR1–REGN5381 (no ANP) map using Phenix[47], producing the model shown in Fig. 2. Cryo-EM data and model statistics are provided in Extended Data Table 1.

Preclinical in vivo mouse studies

***NPR1*$^{hu/hu}$ mice.** *NPR1*$^{hu/hu}$ mice were generated on the C57BL/6NTac (75%)/129S6SvEvTac (25%) background using the Velocigene platform[48]. The generation of these mice was necessitated by the poor conservation of the NPR1 amino acid sequence between human and mouse, and the need to generate a human antibody. Each animal was implanted with PA-C10 (Data Sciences) radiotelemetry devices for the recording of central arterial pressures. The transmitter was located in the carotid artery of each mouse.

All of the mouse experiments were conducted in compliance with protocols approved by the Regeneron Pharmaceuticals Institutional Animal Care and Use Committee, in accordance with state and federal guidelines. Mice were fed normal chow (PicoLab Rodent Diet 20, 5001), housed under standard conditions and allowed to acclimatize for at least 7 days before being placed on the study.

REGN5381 was diluted with sterile phosphate-buffered saline for subcutaneous injection into mice.

REGN5381 single-dose mouse study. Telemetered *NPR1*$^{hu/hu}$ mice were randomly assigned to one of five dosing groups (n = 4–6 per group) on the basis of body weight, and received a single subcutaneous dose of saline or REGN5381 (1, 5, 25 or 50 mg per kg) on study day 0. The BP of each animal was continuously monitored for 28 days. Urine samples for urinalysis and urinary biomarkers were collected on day 28 after dosing.

REGN5381 versus standard-of-care therapies. Comparisons of REGN5381 alone and in combination with standard-of-care therapies

were conducted as a series of four separate experiments. For each experiment, telemetered *NPR1*$^{hu/hu}$ mice were stratified by systolic BP into one of four dosing groups (n = 5–7 per group). The groups then received a single subcutaneous dose of saline or REGN5381 (25 mg per kg), immediately followed by an oral gavage dose of water or standard-of-care therapy (enalapril 25 mg per kg per day; valsartan 125 mg per kg per day; sacubitril 120 mg per kg per day; sildenafil 40 mg per kg per day; milrinone 5 mg per kg per day; propranolol 5 mg per kg per day; nifedipine 20 mg per kg per day; sacubitril/valsartan 100 mg per kg; empagliflozin 30 mg per kg; spironolactone 100 mg per kg). Oral dosing continued once daily in the morning for 7 days. The dose volume for each animal was based on the most recent body weight measurement. Each animal's BP was continuously monitored for 7 days.

Ex vivo vessel reactivity. *NPR1*$^{hu/hu}$ mice were euthanized by CO_2 inhalation followed by laparotomy. The abdominal aorta, third-order mesenteric arteries and mesenteric vein were dissected. Arterial and vein segments (~2 mm in length) were placed into ice-cold Krebs buffer solution and prepared for wire myography. Vascular rings were mounted onto wires in the chambers of a multivessel myograph (J P Trading) filled with Krebs buffer maintained at 37 °C (refs. 49–51). The buffer was gassed with 95% O_2–5% CO_2. After equilibration for 30–60 min, the vessels were set to an internal circumference equivalent to 90% of what they would be in vivo when relaxed under an intraluminal pressure of 100 mm Hg (ref. 49). Isometric tension was monitored continuously before and after experimental interventions and was expressed as mN mm^{-1} vessel length. The experiments were initiated after a 30–60 min stabilization interval. In each vessel, the constrictor response to 80 mmol l^{-1} KCl was determined. Vessels were precontracted with phenylephrine (10×10^{-6} mol l^{-1}), and the vasodilatory response to acetylcholine or test article was measured. Data were expressed as mean ± s.e.m. Concentration–response data derived from each vessel was fitted separately to a logistic function by nonlinear regression, and the maximum asymptote of the curve (maximal response) and concentration of agonist producing EC_{50} were calculated using commercially available software (GraphPad Prism v.9.0.2). Concentration–response data were analysed using two-way analysis of variance followed by Tukey's test. All other data were analysed using one-way analysis of variance or the Student's t-tests for unpaired samples.

Non-human primate pharmacodynamic study. Thirty cynomolgus monkeys (*Macaca fascicularis*) of Mauritius origin, 2–4 years of age and weighing 3–5 kg (Charles River Laboratories), were enrolled in the study. Each animal was implanted with PhysioTel Digital model L11 (Data Sciences International) radiotelemetry devices for recording the central arterial pressure and ECG waveforms. The transmitter was located intramuscularly in a dorsal position and lateral to the median plane below the ribs, and the attached BP catheter was located in the femoral artery with the tip of the catheter located in the descending aorta.

The animals were acclimatized to laboratory housing for a minimum of 5 weeks before initiation of dosing (including recovery time after surgical implantation when performed). During treatment, non-human primates were housed individually in stainless-steel cages in a controlled environment under standard conditions. They were provided Purina Certified Primate Diet 5048 biscuits twice daily and assorted fresh fruit or vegetables. Reverse-osmosis-filtered water was provided ad libitum by means of an automatic watering system. All non-human primate experiments were conducted in compliance with protocols approved by the Charles River Institutional Animal Care and Use Committee, in accordance with state and federal guidelines.

Telemetered animals were randomly assigned to one of six dosing groups (n = 5 per group) and received a single subcutaneous dose of saline or REGN5381 (1, 5 or 25 mg per kg bolus), or a single intravenous dose of REGN5381 (5 or 25 mg per kg bolus) on study day 1. Each animal's BP was continuously monitored for 28 days, and thereafter once weekly for 24 h until the completion of the study on day 56. Urine samples for urinalysis and urinary biomarkers were collected from a cage pan in the morning at baseline and 24 h after dosing. Blood samples for clinical chemistry and the determination of systemic REGN5381 concentrations in the serum were collected from all animals before dosing, and on days 2, 3, 4, 7, 14, 28, 42 and 56 after dosing. Blood samples collected at predose and on day 56 were also analysed for ADA. Concentrations of total REGN5381 (all drugs; without regard to binding site occupancy) were determined using an enzyme-linked immunosorbent assay. ADA analysis was conducted using a generic immunoassay against anti-human IgG4 antibodies.

Canine telemetry study. Two beagle canines (*Canis lupus familiaris*) 8–10 months of age and weighing 9–10.5 kg were received from Marshall BioResources and enrolled in the study. For telemetry studies, each animal was implanted with PhysioTel Digital model D70 (Data Sciences) radiotelemetry devices for recording the central arterial pressure.

Animals were acclimatized to the laboratory housing for a minimum of 2 weeks before initiation of dosing (including recovery time after surgical implantation when performed). During treatment, canines were housed in groups of two in a controlled environment under standard conditions. They were provided PMI Nutrition international Certified Canine LabDiet 5007 daily. Reverse-osmosis-filtered water was provided ad libitum. All canine experiments were conducted in compliance with protocols approved by the Charles River Institutional Animal Care and Use Committee, in accordance with state and federal guidelines.

A cross-over design was used, and each canine received a single intravenous bolus dose of saline (control, n = 2), followed by a 7-day washout period. Canines then received a single intravenous slow bolus of 25 mg per kg REGN5381 (n = 2). Radiotelemetry data were acquired continuously, beginning 48 h before the first administration of vehicle or REGN5381, and continued for 48 h after dosing.

Acute anaesthetized canine study. Twelve beagle canines (*C. l. familiaris*) 11–13 months of age and weighing 9–15 kg were received from Covance and enrolled in the study. General procedures for animal care and housing met current American Association for Accreditation of Laboratory Animal Care International recommendations, Guide for the Care and Use of Laboratory Animals and the US Department of Agriculture through the Animal Welfare Act (as amended, and conformed to testing facility SOP)[52,53]. Canines were housed in runs (up to two canines per run). The temperature and humidity ranges of the study room were set to maintain 74 ± 10 °F and 50 ± 20%, respectively. The light cycle was set to maintain 12 h–12 h on–off. Canines were offered Certified Canine Diet (LabDiet 5007) once daily except on the day of that canine's scheduled experiment; each canine was kept on an overnight fast before the day of its scheduled experiment. Canines were provided with fresh water ad libitum using an automatic watering system except when removed from the run. Anaesthetized canines were instrumented with venous and arterial catheters. Each canine received a single intravenous bolus dose of saline (control, n = 6) or 25 mg per kg REGN5381 (n = 6). Following dose administration, canines were monitored for acute haemodynamic changes.

Before dose administration, each canine was anaesthetized and instrumented for cardiovascular data collection. After placement of all cardiovascular instrumentation, each canine had baseline haemodynamic parameters collected before dosing while they were anaesthetized. Each dose was administered as a single intravenous bolus to the animal. Dose volumes were based on each canine's most recent individual body weight. After dose administration, the animals were monitored for acute haemodynamic changes. Throughout each experiment, blood and urine samples, as well as haemodynamic parameters, were collected.

Canine surgical catheter implantation. A minimum of two venous catheters were placed into a peripheral vessel (for example, cephalic and/or saphenous) for administration of anaesthetics and analgesics. General anaesthesia was induced intravenously (bolus) with propofol (approximately 6 mg per kg) and α-chloralose (30–100 mg per kg), aided by fentanyl (approximately 5 μg per kg). A cuffed endotracheal tube was placed and used to mechanically ventilate the lungs with up to 100% O_2 through a volume-cycled animal ventilator (10–15 breaths per min with a tidal volume of 15–30 ml per kg) to sustain end-tidal expired CO_2 values within the normal physiological range (35–45 mm Hg). Anaesthesia was maintained by intravenous infusion of α-chloralose (20–55 mg per kg per h), with analgesia provided by intravenous infusion of fentanyl (2.0–10.0 μg per kg per h) to preserve normal autonomic function, as well as inotropic/lusitropic properties. Fentanyl and α-chloralose infusions ran concurrently through the same, single peripheral venous catheter. The second venous catheter was used for dosing of control/test article. Surface electrodes were placed onto the thorax for the recording of body-surface ECGs (for example, Lead II). The body temperature was maintained within the normal physiological range by temperature-controlled warming blankets.

Local anaesthesia (bupivacaine 0.5%, 1–2 ml per site) was administered subcutaneously over each surgical site before surgical manipulation. Once a surgical plane of anaesthesia was achieved, a cut-down over a jugular vein and carotid artery was performed for placement of fluid-filled introducers. Two vessel introducers were secured within the jugular vein/jugular vein branches. Through one of the jugular access catheters, a flow-directed Swan Ganz sampling catheter was advanced into the pulmonary artery for the determination of pulmonary artery pressures, right atrial pressures/CVPs. Through the carotid artery, a catheter was advanced into the left ventricle for assessment of left ventricular pressure. A cut-down over the femoral triangle was used to access the femoral artery and vein. A fluid-filled introducer was secured within the femoral artery; through this femoral artery introducer, a solid-state pressure transducer was advanced into the artery to collect an arterial pressure waveform.

ANP and BNP expression constructs. The mouse BNP hydrodynamic delivery construct was constructed by ligating synthetic DNA constructs (Genscript) containing the *Nppb* coding sequences through the BglII–NotI restriction sites into the vector pRG977-mRor-V5 (N-term.) to create the final constructs used for injection into mice. The reference sequence used in the design of the expression construct was mouse *Nppb* reference protein (NCBI: NP_032752). The mouse ANP hydrodynamic delivery construct was constructed by ligating synthetic DNA constructs (Genscript) containing the *Nppa* coding sequences into the vector pRG977 to create the final constructs used for injection into mice. The reference sequence used in the design of the expression construct was mouse *Nppa* reference protein (NP_032751). On study day 0, mice were stratified into groups on the basis of body weight. Mice were injected through the tail vein with 50 μg plasmid in sterile saline at 10% of body weight.

Clinical study

REGN5381 in a first-in-human study. A phase 1, double-blind, placebo-controlled, two-part single-ascending dose study was designed to assess the safety, tolerability and pharmacodynamics/pharmacokinetics of REGN5381 in healthy adults (18–55 years of age; NCT04506645). Data reported here include only findings from the first part, which was conducted in healthy adults (18–55 years of age) at a single site. The study protocol was approved by institutional review boards or relevant ethics committee, and the research ethics committee of the University Hospitals of Leuven. The study was conducted in accordance with the ethical principles originating from the Declaration of Helsinki, and was consistent with the International Conference on Harmonization/Good Clinical Practices and applicable regulatory requirements. All of the participants provided written informed consent.

Participants were screened for systolic BP 100–140 mm Hg (inclusive) and diastolic BP 60–90 mm Hg (inclusive). If the participants in a dosing cohort experienced clinically important hypotension or tachycardia, the BP inclusion criteria could be adapted to allow for increases in the range (systolic BP, 130–165 mm Hg; diastolic BP, 60–100 mm Hg), although adaptation of the inclusion criteria was not necessary. After initial screening, the participants attended a 2-day inpatient treatment/observation period before dosing and were placed on a fixed-sodium diet to ensure consistency in sodium intake and to reduce the variability in BP due to dietary sodium. Non-invasive haemodynamics were measured using pulse-wave analysis technology (ClearSight, Edwards Lifesciences) beginning 1 day before randomization and continued through to the end of the inpatient monitoring period.

The participants were randomized 6:2 to receive single-dose intravenous REGN5381 (0.3, 1, 3, 10, 30 or 100 mg) or intravenous placebo. After study drug administration on day 1, the participants remained in the clinic until day 4 to allow careful monitoring of haemodynamics. On day 4, the participants were assessed for safety before discharge. The study duration was based on predicted blood levels of REGN5381 concentrations in the serum across all dose cohorts; the end of the study visit was conducted no earlier than 21 days after the administration of the study drug. The primary end point in this study was the type, incidence and severity of TEAEs after a single intravenous dose administration of REGN5381 or placebo over time.

Statistical analyses

Preclinical assessments. Statistical analysis was performed using standard statistical software (GraphPad Prism 7). Analysis of data were performed using one-way analysis of variance or two-way repeated-measures analysis of variance. Tukey's post hoc multiple-comparison test ($\alpha = 0.05$) was used. Data are reported as mean ± s.e.m. $P < 0.05$ was considered to be significant.

First-in-human clinical assessments. There was no formal primary efficacy analysis in this study. For continuous variables, descriptive statistics included the following information: the number of participants reflected in the calculation (n), mean, s.d., quartile 1, quartile 3, median, minimum and maximum. Plots of the values over time, as well as the change or percentage change over time, were provided.

Haemodynamic parameters are known to be sensitive to the nominal time of the day; for example, a participant may have a relatively higher BP during the daytime than at night. Thus, a time-matched change from baseline in systolic BP, diastolic BP, mean arterial pressure, pulse pressure and cardiac stroke volume across the first 24 h after dose was reported by treatment group. For example, the time-matched change from baseline at 07:00 was calculated as follows:

$$\mathrm{Chg}_{07:00} = \mathrm{BP}_{07:00\,\mathrm{D1}} - \mathrm{BP}_{07:00\,\mathrm{D-1}}$$

where $\mathrm{BP}_{07:00\,\mathrm{D1}}$ was the BP collected at 07:00 on day 1 and $\mathrm{BP}_{07:00\,\mathrm{D-1}}$ was the blood pressure collected at 07:00 on day −1. Time-matched mean change from the baseline for the pulse-wave analysis was provided by treatment group.

For categorical or ordinal data, frequencies and percentages were displayed for each category. Unless otherwise specified, the participants randomized to placebo were pooled across cohorts.

Reporting summary

Further information on research design is available in the Nature Portfolio Reporting Summary linked to this article.

Data availability

Researchers may request access to study documents (including the clinical study report, study protocol with any amendments, blank case report form and statistical analysis plan) supporting the methods and findings reported in this Article. Individual anonymized participant data will be considered for sharing (1) once the product and indication have been approved by major health authorities (such as the FDA, EMA, PMDA) or development of the product has been discontinued globally for all indications on or after April 2020 and there are no plans for future development; (2) if there is legal authority to share the data; and (3) if there is not a reasonable likelihood of participant re-identification. Submit requests to https://vivli.org/.

32. Backman, J. D. et al. Exome sequencing and analysis of 454,787 UK Biobank participants. *Nature* **599**, 628–634 (2021).
33. Verweij, N. et al. Germline mutations in *CIDEB* and protection against liver disease. *N. Engl. J. Med.* **387**, 332–344 (2022).
34. Tobin, M. D., Sheehan, N. A., Scurrah, K. J. & Burton, P. R. Adjusting for treatment effects in studies of quantitative traits: antihypertensive therapy and systolic blood pressure. *Stat. Med.* **24**, 2911–2935 (2005).
35. Evangelou, E. et al. Genetic analysis of over 1 million people identifies 535 new loci associated with blood pressure traits. *Nat. Genet.* **50**, 1412–1425 (2018).
36. Sun, B. B. et al. Genetic regulation of the human plasma proteome in 54,306 UK Biobank participants. Preprint at *bioRxiv* https://doi.org/10.1101/2022.06.17.496443 (2022).
37. Taliun, D. et al. Sequencing of 53,831 diverse genomes from the NHLBI TOPMed Program. *Nature* **590**, 290–299 (2021).
38. Das, S. et al. Next-generation genotype imputation service and methods. *Nat. Genet.* **48**, 1284–1287 (2016).
39. Fuchsberger, C., Abecasis, G. R. & Hinds, D. A. minimac2: faster genotype imputation. *Bioinformatics* **31**, 782–784 (2015).
40. Akbari, P. et al. Sequencing of 640,000 exomes identifies GPR75 variants associated with protection from obesity. *Science* **373**, eabf8683 (2021).
41. Akbari, P. et al. Multiancestry exome sequencing reveals INHBE mutations associated with favorable fat distribution and protection from diabetes. *Nat. Commun.* **13**, 4844 (2022).
42. Mbatchou, J. et al. Computationally efficient whole-genome regression for quantitative and binary traits. *Nat. Genet.* **53**, 1097–1103 (2021).
43. Johnsson, B., Lofas, S. & Lindquist, G. Immobilization of proteins to a carboxymethyldextran-modified gold surface for biospecific interaction analysis in surface plasmon resonance sensors. *Anal. Biochem.* **198**, 268–277 (1991).
44. Myszka, D. G. Improving biosensor analysis. *J. Mol. Recognit.* **12**, 279–284 (1999).
45. Punjani, A., Rubinstein, J. L., Fleet, D. J. & Brubaker, M. A. cryoSPARC: algorithms for rapid unsupervised cryo-EM structure determination. *Nat. Methods* **14**, 290–296 (2017).
46. Emsley, P. & Cowtan, K. Coot: model-building tools for molecular graphics. *Acta Crystallogr. D* **60**, 2126–2132 (2004).
47. Afonine, P., Headd, J., Terwilliger, T. & Adams, P. New tool: phenix.real_space_refine. *Comput. Crystallogr. Newsl.* **4**, 43–44 (2013).
48. Valenzuela, D. M. et al. High-throughput engineering of the mouse genome coupled with high-resolution expression analysis. *Nat. Biotechnol.* **21**, 652–659 (2003).
49. Mulvany, M. J. & Halpern, W. Contractile properties of small arterial resistance vessels in spontaneously hypertensive and normotensive rats. *Circ. Res.* **41**, 19–26 (1977).
50. Zhang, F. et al. Decreased levels of cytochrome P450 2E1-derived eicosanoids sensitize renal arteries to constrictor agonists in spontaneously hypertensive rats. *Hypertension* **45**, 103–108 (2005).
51. Zhang, F. et al. CO modulates pulmonary vascular response to acute hypoxia: relation to endothelin. *Am. J. Physiol. Heart Circ. Physiol.* **286**, H137–H144 (2004).
52. US Department of Agriculture. *Animal Welfare Act and Animal Welfare Regulations* (USDA, 2019); www.aphis.usda.gov/animal_welfare/downloads/bluebook-ac-awa.pdf.
53. National Research Council of the National Academies. *Guide For The Care Of and Use Of Laboratory Animals* 8th edn (National Academies Press, 2011); grants.nih.gov/grants/olaw/guide-for-the-care-and-use-of-laboratory-animals.pdf.

Acknowledgements We thank the participants, their families and all investigators and personnel from the Center for Clinical Pharmacology involved in this study; the Regeneron Genetics Center (RGC) authors who contributed towards this study—a complete list of RGC authors and their contributions is provided; all Regeneron employees who contributed to the generation and characterization of REGN5381, including P. Molina, Hock E., R. Babb, J. Martin, L. Collins, S. Veerasammy, K. Hofmeyer and A. Solorzan; T. Chen for his contributions; S. Tichenor and the expert staff of Charles River Labs, Reno, Nevada, for their large animal pharmacology study support; R. Hamlin, B. Youngblood and W. Muir of QTest Labs for their large-animal cardiovascular haemodynamic study support; and M. Schwartzman and F. F. Zhang for their support with the vessel ring studies. The U.K. Biobank resource (26041) was used in this research. Indiana Biobank is supported in part by UL1TR002529. Medical writing support was provided by R. Dessai of Alpha (a division of Prime, Knutsford, UK), supported by Regeneron Pharmaceuticals, according to good publication practice guidelines. The sponsor was involved in the study design and collection, analysis and interpretation of data, as well as data checking of information provided in the Article. This study was funded and supported by Regeneron Pharmaceuticals.

Author contributions All of the authors contributed to the collection of data, interpretation of results, critical review of the manuscript for important intellectual content and final approval of submission of the manuscript for publication. J.B.N., T.D., N.V., A.P., A.L., A.B. and L.A.L. supported the human genetics experimental design, analysis and interpretation. J.H.K., A.J.-H.H., M.C.F., A.R.H., V.K., E.G., N.L., M.R., S.K., M.E.B., T.H. and W.O. supported the in vitro experimental design, analysis and interpretation. M.E.D., A.K., X.J., D.Z., J.T., D.J., H.P., J.M., K.B.D.-N., B.A.O. and L.M. supported the in vivo experimental design, analysis and interpretation. M.E.D., A.K., J. Mastaitis, J.d.H., W.B., W.Z., B.J.M., G.H., G.D.Y. and B.A.O. supported the execution of clinical studies and analysed data. W.Z. and B.M. interpreted data analysis. M.E.D., K.B.D.-N., A.R., W.O., T.H., G.H., A.J.M., G.D.Y., B.A.O., L.M. and B.J.M. supervised the studies and helped with interpretation. M.E.D., A.K., J.H.K., M.C.F. and J.B.N. wrote the manuscript. Contributions for the Regeneron Genetics Center were as follows. Leadership and management: G.A., A.B., M.C., G.C., A.D., A.E., L.A.L., J.D.O., J.G.R., K.S. and A.S. Sequencing and laboratory operations: C.B., C.F., E.D.F., Z.G., M.L., A.L., J.D.O., M.S.P., M.P., K.M., T.D.S., L.W., S.E.W. and R.H.U. Clinical informatics: A.A., N.B., M.C., D.L., S.M., D.S. and J.C.S. Genome informatics: X.B., S.B., S.B, B.B., S.C., G.E., L.H., A.H., S.K., O.K., R.L., A.J.M., E.K.M., G.M., M.N., S.O., M.O., R.P., T.P., A.R., J.G.R., W.S., J.C.S. and K.S. Analytical genomics and data science: G.A., J.B., A.D., L.D., M.A.R.F., A.G., C.G., L.G., E.J., H.M.K., M.K., J.K., A.L., N.L., D.L., A.L., J. Meyer, A.M., J. Mastaitis, A.M., C.P., C.S., E.S., K.W., B.Y., B.Z. and A.Z. Therapeutic area genomics: A.A., A.G., G.H., G.C., J.F., J.B., K.S., K.P., L.A.L., M.K., M.H., M.R., N.V., O.S., P.A., P.N., S.G., S.G., T.D., V.R., A.S., B.Y., G.T. and J.R.-F. Research programme management and research initiatives: E.C., M.B.J., M.G.L., J. Mastaitis, L.J.M., N.N., N.R., J.H. and J.R.V. Contributions for the Penn Medicine Biobank were as follows. D.J.R. and M.D.R. contributed to securing funding, study design and oversight, as well as reviewing and approving the final version of the manuscript. J.W. managed recruitment and regulatory oversight of the study. N.N. managed participant engagement, assisted with regulatory oversight and research access. A.P., K.H. and Y.K. performed recruitment and enrolment of study participants. J.W., M.L., F.V. and S.D. conducted oversight of laboratory operations. M.L., F.V., A.K., S.D., T.T., J.S. and M.Z. performed sample processing. N.H. and J.D. were responsible for sample tracking and the laboratory information management system. A.V., C.M.K., M.R. and R.J. contributed to the development and validation of clinical phenotypes used to identify study participants and (when applicable) controls. A.V. and S.S.V. were responsible for the analysis, design and infrastructure needed to quality-control genotype and exome data. Y.B. performed the analysis. T.D. and A.V. provided variant and gene annotations and their functional interpretation of variants. All of the team members of the GHS-RGC DiscovEHR Collaboration were collectively instrumental in recruiting participants, sample collection, extraction of phenotype data and contributors to feedback on genetic results.

Competing interests M.E.D., A.K., J.H.K., A.J.-H.H., M.C.F., X.J., D.Z., J.T., E.G., N.L., M.R., H.P., S.K., M.E.B., W.Z., A.R., J.B.N., T.D., N.V., A.P., A.L., A.B., L.A.L., B.J.M., J. Mastaitis, K.B.D.-N., T.H., G.H., W.O., A.J.M., G.D.Y., B.A.O. and L.M. are employees of and shareholders in Regeneron Pharmaceuticals. A.R.H., J. Meyer, D.J., V.K. and A.J.R. were employees of Regeneron Pharmaceuticals at the time of the studies. The other authors declare no competing interests.

Additional information

Supplementary information The online version contains supplementary material available at https://doi.org/10.1038/s41586-024-07903-1.

Correspondence and requests for materials should be addressed to Michael E. Dunn.

Peer review information *Nature* thanks Lincoln Potter and the other, anonymous, reviewer(s) for their contribution to the peer review of this work.

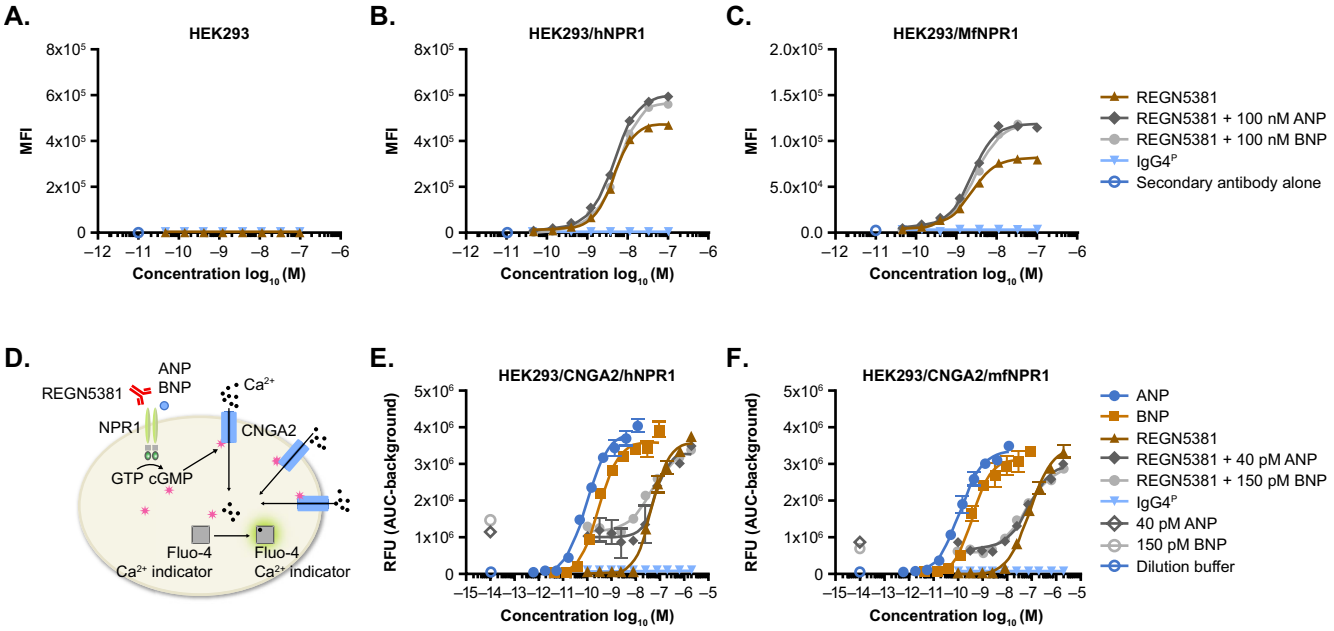

Extended Data Fig. 1 | REGN5381 binds and activates NPR1 in the presence or absence of natriuretic peptide ligands. A–**C**, Specific binding of REGN5381 to human and cynomolgus monkey NPR1 was tested with **A**, HEK293, **B**, HEK293/hNPR1, and **C**, HEK293/MfNPR1 cells by flow cytometry. REGN5381 binds to **B**, hNPR1 with EC_{50} values of 4.58 nM (no ligand), 4.56 nM (with 100 nM ANP) and 5.69 nM (with 100 nM BNP) and **C**, mfNPR1 EC_{50} values of 2.27 nM (no ligand), 2.42 nM (100 nM ANP) and 3.01 nM (with 100 nM BNP). Key: brown solid triangles, REGN5381; dark grey solid diamonds, REGN5381 + 100 nM ANP; grey solid circles, REGN5381 + 100 nM BNP; blue solid triangle, $IgG4^P$; blue open circle, antibody control. **D**, schematic diagram of calcium flux assay measuring calcium mobilization through CNGA2 channel upon ligand or REGN5381-induced NPR1 activation. **E**, REGN5381 activated hNPR1 with EC_{50} values of 46.8 nM (no ligand), 68.1 nM (40 pM ANP) and 42.5 nM (150 pM BNP) as measured by calcium flux assay with and HEK293/CNGA2/hNPR1. **F**, mfNPR1 with EC_{50} values of 82.2 nM (no ligand), 81.7 nM (40 pM ANP) and 57.5 nM (150 pM BNP) with HEK293/CNGA2/mfNPR1 cells. Open symbols indicate conditions when no test article was added, and closed symbols indicate conditions when the test article was added in a range of concentrations. Key: blue solid circles, ANP; light brown solid square, BNP; brown solid triangle, REGN5381; dark grey solid diamond, REGN5381 + 40 pM ANP; grey solid circle, REGN5381 + 150 pM BNP; blue solid triangle, $IgG4^P$; dark grey open diamond, 40 pM ANP; grey open circle, 150 pM BNP; blue open circle, dilution buffer control. REGN5381 binds to cells expressing human NPR1 (hNPR1) and monkey NPR1 (mfNPR1) in the absence of ligand, and binding is enhanced in the presence of ANP and BNP. ANP, atrial natriuretic peptide; AUC, area under the curve; BNP, brain natriuretic peptide; CNGA2, cyclic-nucleotide-gated calcium channels; GTP, guanosine triphosphate; $IgG4^P$, non-binding immunoglobulin G control; MFI, mean fluorescence intensity; NPR1, natriuretic peptide receptor 1; RFU, relative fluorescence units.

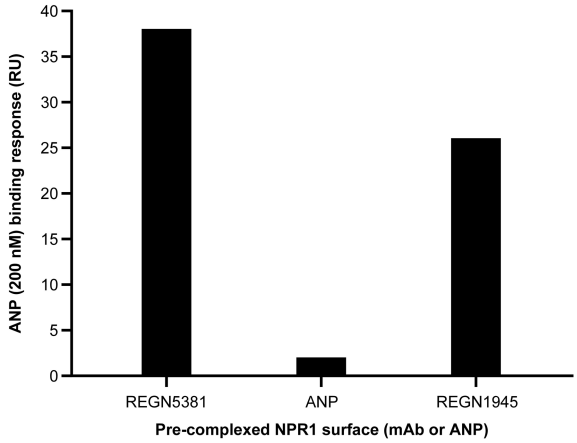

Extended Data Fig. 2 | REGN5381 does not inhibit ANP binding to NPR1. ANP binding in the presence of antibody was tested using Biacore S200. Human NPR1-mmh protein was captured over anti-His coated Biacore coupled chip for 10 min. NPR1 captured chip was first saturated with REGN5381 or IgG4 control antibody at 50 ug/ml or 200 nM of ANP for 4 min followed by testing with second injection of 200 nM ANP for 4 min over each complex NPR1 surface. The ANP binding response was recorded after the second injection and it showed that REGN5381 does not block ANP binding to NPR1-mmh. ANP, atrial natriuretic peptide; IgG4, immunoglobulin G; mab, monoclonal antibody; NPR1, natriuretic peptide receptor 1.

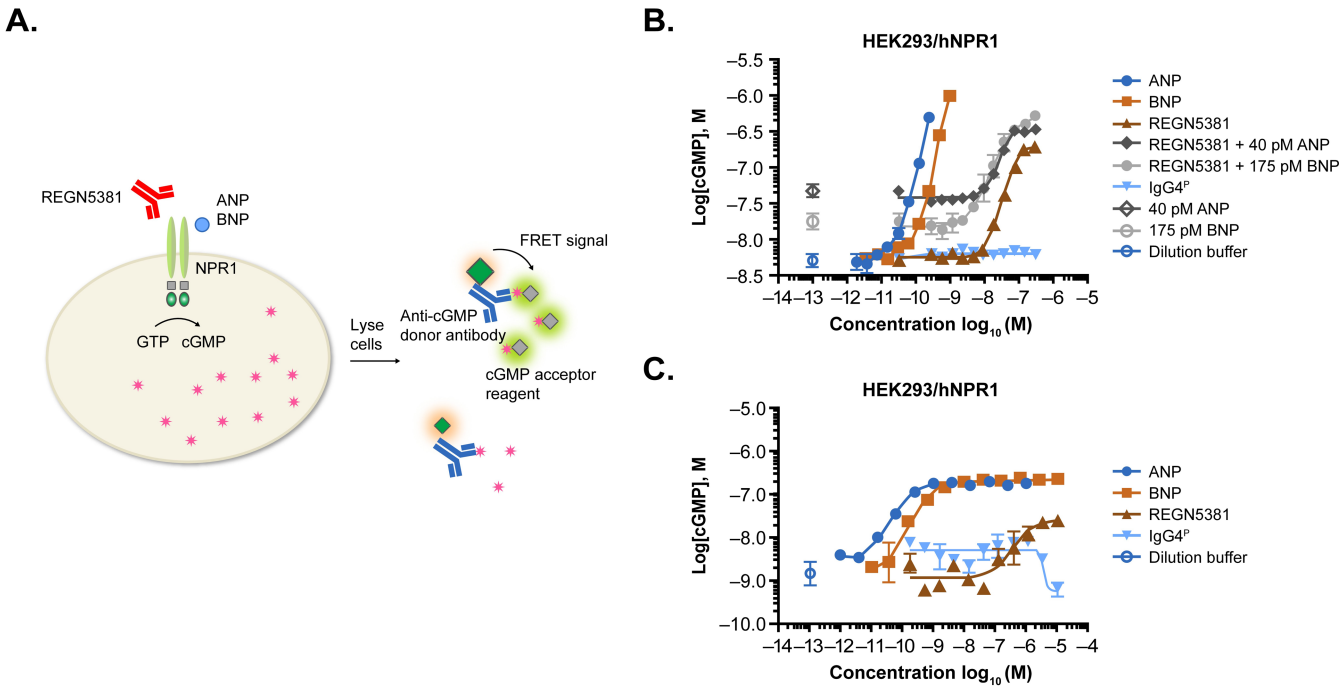

Extended Data Fig. 3 | REGN5381 activated human NPR1-mediated cGMP production. A, Schematic diagram of cGMP accumulation assay measuring hNPR1 activation-induced cGMP production. **B, C**, The activity of REGN5381 and ligand at hNPR1 was measured with HEK293/hNPR1 cells using different conditions due to the limit of quantitation for ligand at high concentrations. **B**, REGN5381 activated hNPR1 in the absence or presence of ligand (ANP or BNP) as measured by cGMP accumulation assays with HEK293/hNPR1 cells. Activation at higher ligand concentrations was seen, but cGMP level was not calculated due to the limit of quantitation. **C**, The full activity of ligand was evaluated with optimized conditions, where REGN5381 exhibited partial agonism compared to the ligand. Open symbols indicate assay conditions when no test article was added, and closed symbols indicate assay conditions when the test article was added in a range of concentrations. Key: blue solid circles, ANP; light brown solid square, BNP; brown solid triangle, REGN5381; dark grey solid diamond, REGN5381 + 40 pM ANP; grey solid circle, REGN5381 + 150 pM BNP; blue solid triangle, IgG4P; dark grey open diamond, 40 pM ANP; grey open circle, 150 pM BNP; blue open circle, dilution buffer control. ANP, atrial natriuretic peptide; BNP, brain natriuretic peptide; cGMP, cyclic guanosine monophosphate; FRET, fluorescence resonance energy transfer; GTP, guanosine triphosphate; hNPR1, human NPR1; IgG4^{P}, non-binding immunoglobulin G control; NPR1, natriuretic peptide receptor 1.

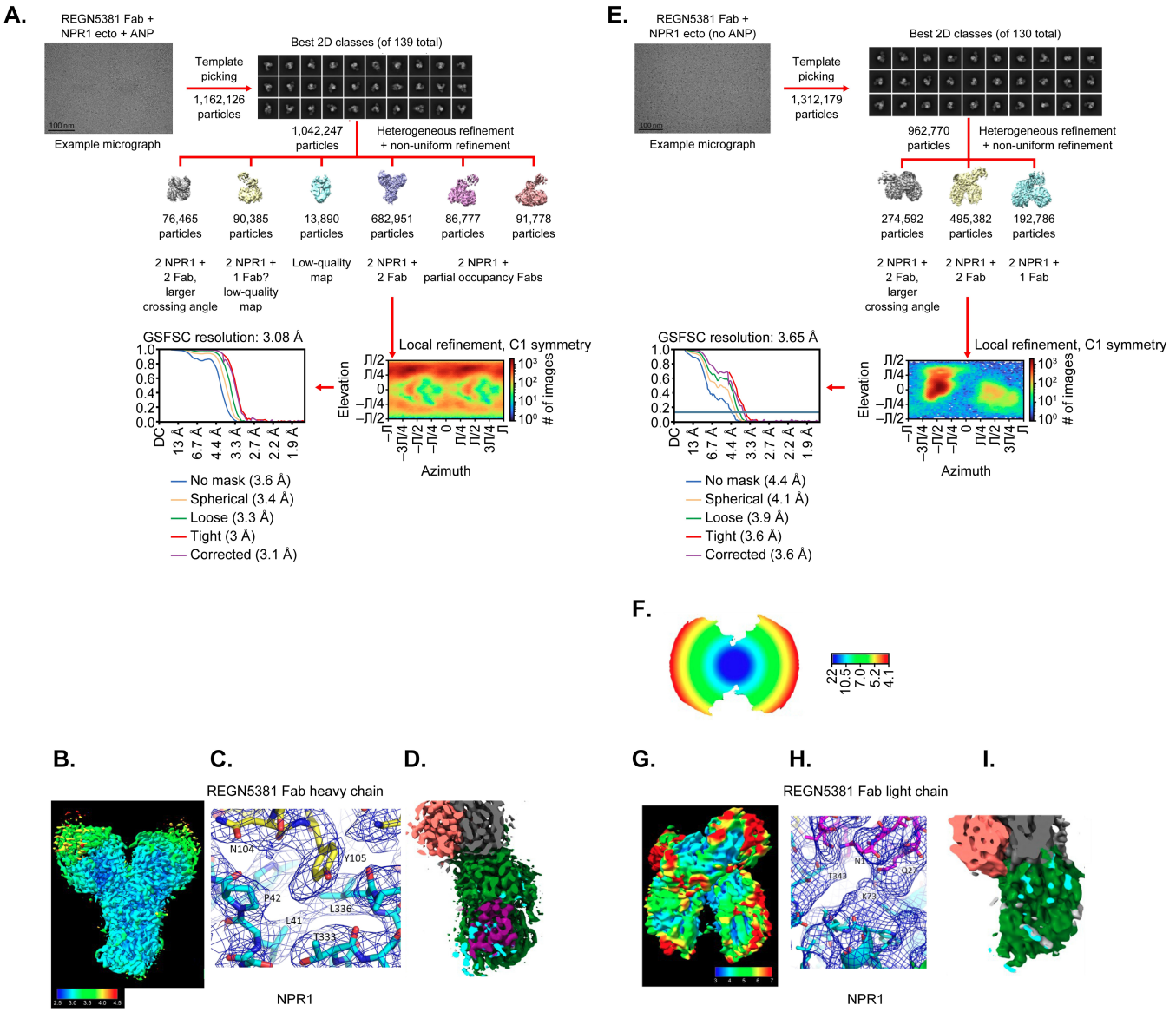

Extended Data Fig. 4 | Cryo-EM data processing. A. Data processing workflow for the REGN5381 Fab + NPR1 ectodomain + ANP complex, including particle orientation distribution and FSC curve for the final reconstruction. **B**. Final map coloured by local resolution, from 2.5 to 5.5 Å. **C**. A sample of the EM density at the NPR1:REGN5381 interface, with selected residues labelled. **D**. A cutaway view of the EM density, sliced through the centre of the dimer to reveal the density at the peptide binding site. Density surface is coloured by molecule: REGN5381 Fab heavy chain – salmon; light chain – grey; NPR1 monomers – green and cyan (mostly hidden); ANP – purple; unassigned density – white. **E**. Data processing workflow for the REGN5381 Fab + NPR1 ectodomain (no ANP) complex. **F**. 3D FSC isosurface at FSC = 0.143, oriented with the lowest resolution along the z axis and the best resolution along the x axis, and coloured radially by resolution as indicated in the colour key. **G**. Local resolution map, oriented to show the absence of the ANP peptide in this complex. **H**. A sample of the EM density for this complex. **I**. A cutaway view of the EM density, sliced through the centre of the dimer to reveal the lack of density at the peptide binding site. Density surface is coloured by molecule: REGN5381 Fab heavy chain – salmon; light chain – grey; NPR1 monomers – green and cyan (mostly hidden); unassigned density – white. ANP, atrial natriuretic peptide; EM, electron microscopy; FSC, Fourier shell correlation; NPR1, natriuretic peptide receptor.

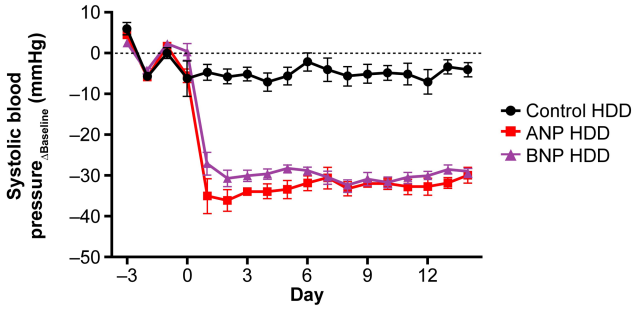

Extended Data Fig. 5 | Hydrodynamic DNA delivery of ANP and BNP expression vectors in normotensive mice induced a sustained reduction in systolic blood pressure. ANP and BNP overexpression resulted in systolic blood pressure reduction of over 30 mmHg. Key: black circles, control; red squares, ANP; purple triangles, BNP. ANP, atrial natriuretic peptide; BNP, brain natriuretic peptide; HDD, hydrodynamic delivery.

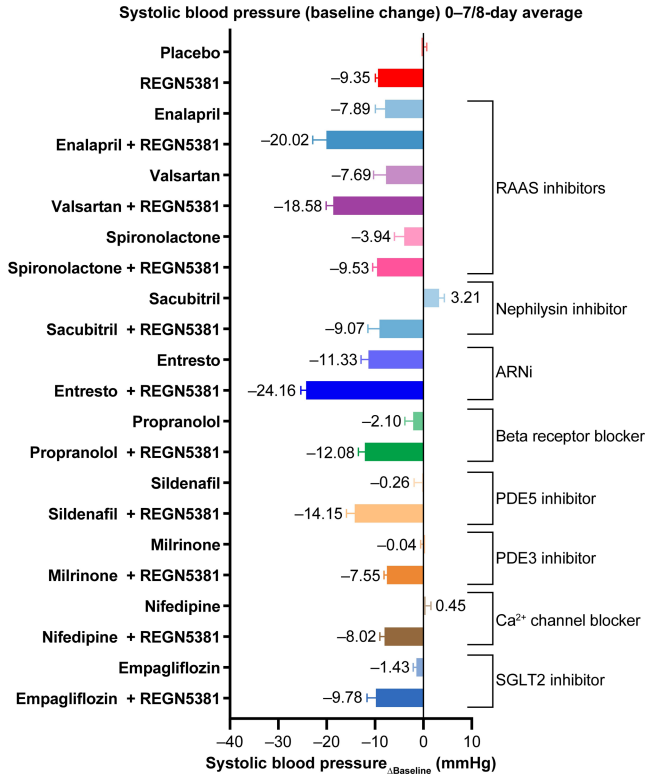

Extended Data Fig. 6 | REGN5381 reduces systolic blood pressure similar to SOC, with additive effects observed upon combination with some but not all SOC therapies. The reduction in systolic blood pressure was assessed in telemetered normotensive NPR1$^{hu/hu}$ mice administered a single subcutaneous dose of REGN5381 either alone or in combination with SOC agents for the treatment of HF and hypertension at therapeutically relevant doses (n = 5–7 per treatment group; pooled placebo n = 36). ARNi, angiotensin receptor/neprilysin inhibitor; HF, heart failure; NPR1, natriuretic peptide receptor; NPR1$^{hu/hu}$, NPR1 humanized; PDE, phosphodiesterase; RAAS, renin-angiotensin-aldosterone system; SGLT2, sodium-glucose cotransporter-2; SOC, standard-of-care.

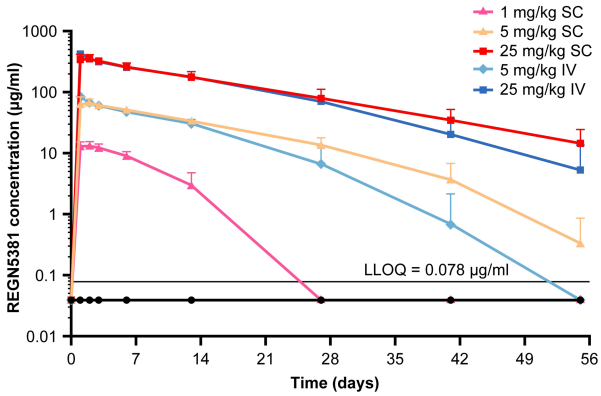

Extended Data Fig. 7 | Mean (+SD) total REGN5381 concentrations in serum vs time following a single subcutaneous or intravenous injection of REGN5381 in normotensive non-human primates. Normotensive cynomolgus monkeys received a single intravenous bolus of saline/vehicle (n = 5; black circles) or REGN5381 subcutaneous (n = 5; 1 mg/kg [pink line]), (n = 5; 5 mg/kg [pale yellow line]), (n = 5; 25 mg/kg [red line]) or intravenous (n = 5; 5 mg/kg [light blue line]) or (n = 5; 25 mg/kg [dark blue line]). Concentrations of total REGN5381 (all drugs; without regard to binding site occupancy) in serum were determined using ELISA. ADA analysis was conducted using a generic immunoassay against anti-human IgG4 antibodies and 32% (8/25) of REGN5381–dosed animals showed a positive response. Nonetheless, all concentration data, regardless of whether potentially impacted by ADA, were included in this plot as the actual exposure would be that used for any correlation with PD effects. ADA, anti-drug antibodies; ELISA, enzyme-linked immunosorbent assay; IgG, immunoglobulin G; IV, intravenous; LLOQ, lower limit of quantification; PD, pharmacodynamics; SC, subcutaneous; SD, standard deviation.

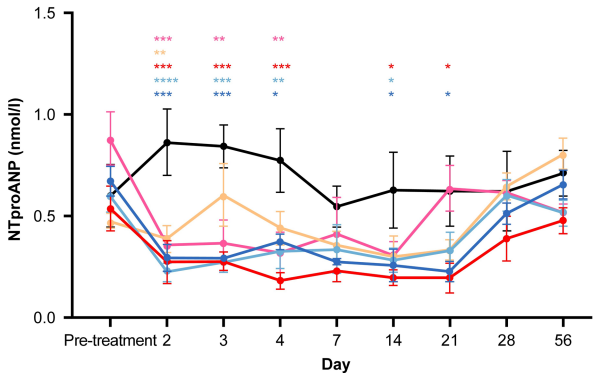

Extended Data Fig. 8 | REGN5381 leads to a reduction of NTproANP in normotensive non-human primates. Normotensive cynomolgus monkeys received a single intravenous bolus of saline/vehicle ($n = 5$; black circles) or REGN5381 subcutaneous ($n = 5$; 1 mg/kg [pink line]), ($n = 5$; 5 mg/kg [pale yellow line]), ($n = 5$; 25 mg/kg [red line]) or intravenous ($n = 5$; 5 mg/kg [light blue line]) or ($n = 5$; 25 mg/kg [dark blue line]). Serum NTproANP levels were measured throughout the study. Data are mean ± SEM. Statistical Analysis: RM 2-Way ANOVA or 1-Way ANOVA; *$p \leq 0.05$; **$p \leq 0.01$; ***$p \leq 0.001$; ****$p \leq 0.0001$. ANOVA, analysis of variance; NTproANP, N-terminal proatrial natriuretic peptide; RM, repeated measures; SEM, standard error of mean; Tx, treatment.

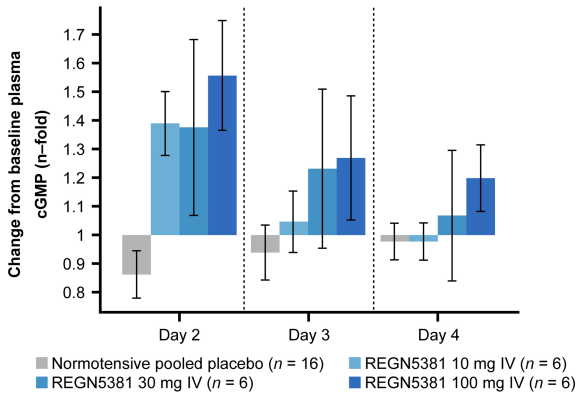

Extended Data Fig. 9 | REGN5381-induced plasma cGMP production in healthy volunteers. Mean ± standard error change from baseline in plasma cGMP levels following administration of study treatment (pooled placebo, grey bar; REGN538110 mg, light blue bar; REGN538130 mg, blue bar; REGN5381 100 mg, dark blue bar). cGMP, cyclic guanosine monophosphate; IV, intravenous; SE, standard error.

Extended Data Table 1 | Cryo-EM data, structure refinement, and validation

	NPR1 ectodomain + ANP + REGN5381	NPR1 ectodomain + REGN5381 (no ANP)
Data collection and processing		
Magnification	105,000	105,000
Voltage (kV)	300	300
Electron exposure (e^{-}/Å^2)	40	41
Defocus range (μm)	-1.0 to -2.5	-1.0 to -2.5
Pixel size (Å)	0.86	0.86
Number of movies	6,717	6,541
Initial number of particles	1.2M	1.3M
Particles selected after 2D classification	1.04M	963K
Final selected particles	682,951	495,382
Symmetry imposed	C1	C1
Map resolution (Å)	3.08	3.65
FSC threshold	0.143	0.143
Refinement		
Initial Model used	1T34	NPR1+ANP+REGN5381 complex (ANP removed)
Model composition		
Non-hydrogen atoms	13,695	13,184
Protein residues	1,726	1,704
N-glycans	15	0
R.m.s. deviations		
Bond lengths (Å)	0.002	0.004
Bond angles (°)	0.469	0.677
Validation		
MolProbity score	1.54	1.64
Rotamer outliers (%)	0.21	0.21
Clash score	5.90	7.12
Ramachandran plot		
Favored (%)	96.6	96.3
Allowed (%)	3.34	3.55
Disallowed (%)	0.06	0.12
Deposition ID		
PDB	8TG9	8TGA
EMDB	EMD-41233	EMD-41234

ANP, atrial natriuretic peptide; EM, electron microscopy; EMDB, electron microscopy data bank; FSC, fourier shell correlation; NPR1, natriuretic peptide receptor 1.

nature portfolio

Corresponding author(s): Dr Michael E. Dunn

Last updated by author(s): Jun 19, 2024

Reporting Summary

Nature Portfolio wishes to improve the reproducibility of the work that we publish. This form provides structure for consistency and transparency in reporting. For further information on Nature Portfolio policies, see our Editorial Policies and the Editorial Policy Checklist.

Statistics

For all statistical analyses, confirm that the following items are present in the figure legend, table legend, main text, or Methods section.

n/a	Confirmed	
☐	☒	The exact sample size (*n*) for each experimental group/condition, given as a discrete number and unit of measurement
☐	☒	A statement on whether measurements were taken from distinct samples or whether the same sample was measured repeatedly
☐	☒	The statistical test(s) used AND whether they are one- or two-sided *Only common tests should be described solely by name; describe more complex techniques in the Methods section.*
☐	☒	A description of all covariates tested
☐	☒	A description of any assumptions or corrections, such as tests of normality and adjustment for multiple comparisons
☐	☒	A full description of the statistical parameters including central tendency (e.g. means) or other basic estimates (e.g. regression coefficient) AND variation (e.g. standard deviation) or associated estimates of uncertainty (e.g. confidence intervals)
☐	☒	For null hypothesis testing, the test statistic (e.g. *F*, *t*, *r*) with confidence intervals, effect sizes, degrees of freedom and *P* value noted *Give P values as exact values whenever suitable.*
☒	☐	For Bayesian analysis, information on the choice of priors and Markov chain Monte Carlo settings
☐	☒	For hierarchical and complex designs, identification of the appropriate level for tests and full reporting of outcomes
☒	☐	Estimates of effect sizes (e.g. Cohen's *d*, Pearson's *r*), indicating how they were calculated

Our web collection on statistics for biologists contains articles on many of the points above.

Software and code

Policy information about availability of computer code

Data collection	Automated data-collection was carried out using EPU (Thermo Fisher Scientific) at a nominal magnification of 105,000x, corresponding to a pixel size of 0.86 Å
Data analysis	Preclinical analysis was performed using standard statistical software (GraphPad Prism 7 and GraphPAD Prism 9.0.2). Genetic analysis was performed using REGENIE version 2+.

For manuscripts utilizing custom algorithms or software that are central to the research but not yet described in published literature, software must be made available to editors and reviewers. We strongly encourage code deposition in a community repository (e.g. GitHub). See the Nature Portfolio guidelines for submitting code & software for further information.

Data

Policy information about availability of data

All manuscripts must include a data availability statement. This statement should provide the following information, where applicable:

- Accession codes, unique identifiers, or web links for publicly available datasets
- A description of any restrictions on data availability
- For clinical datasets or third party data, please ensure that the statement adheres to our policy

Qualified researchers may request access to study documents (including the clinical study report, study protocol with any amendments, blank case report form, statistical analysis plan) that support the methods and findings reported in this manuscript. Individual anonymized participant data will be considered for sharing

once the product and indication has been approved by major health authorities (e.g. FDA, EMA, PMDA, etc.) or development of the product has been discontinued globally for all indications on or after April 2020 and there are no plans for future development, (2) if there is legal authority to share the data and (3) there is not a reasonable likelihood of participant re-identification. Submit requests to https://vivli.org/.

PDB codes: 1T34, 1DP4

Research involving human participants, their data, or biological material

Policy information about studies with human participants or human data. See also policy information about sex, gender (identity/presentation), and sexual orientation and race, ethnicity and racism.

Reporting on sex and gender	The findings are applicable to all sexes and genders. No sex- or gender-based analyses have been performed.
Reporting on race, ethnicity, or other socially relevant groupings	No race, ethnicity, or other socially relevant groupings based analyses have been performed.
Population characteristics	Healthy male or female adults 18 to 55 years of age (inclusive) were included in the clinical study. Participants were screened for systolic BP 100–140 mmHg (inclusive) and diastolic BP 60–90 mmHg (inclusive). If participants in a dosing cohort experienced clinically significant hypotension or tachycardia, the BP inclusion criteria could be adapted to allow for increases in the range (systolic BP, 130–165 mmHg; diastolic BP, 60–100 mmHg), though adaptation of the inclusion criteria was not necessary. After initial screening, participants attended a 2-day inpatient treatment/observation period prior to dosing and were placed on a fixed-sodium diet to ensure consistency in sodium intake and to reduce the variability in BP due to dietary sodium. Noninvasive hemodynamics were measured using pulse wave analysis technology (ClearSight, Edwards Lifesciences) beginning 1 day prior to randomization and continued through to the end of the inpatient monitoring period.
Recruitment	Participants were recruited at a single site (Belgium). There was no selection bias in recruitment of patients in the trial.
Ethics oversight	The study protocol was approved by institutional review boards or relevant ethics committee, and the research ethics committee of the University Hospitals of Leuven. The study was conducted in accordance with the ethical principles originating from the Declaration of Helsinki, and was consistent with the International Conference on Harmonization/Good Clinical Practices and applicable regulatory requirements.

Note that full information on the approval of the study protocol must also be provided in the manuscript.

Field-specific reporting

Please select the one below that is the best fit for your research. If you are not sure, read the appropriate sections before making your selection.

☒ Life sciences ☐ Behavioural & social sciences ☐ Ecological, evolutionary & environmental sciences

For a reference copy of the document with all sections, see nature.com/documents/nr-reporting-summary-flat.pdf

Life sciences study design

All studies must disclose on these points even when the disclosure is negative.

Sample size	A total of 48 healthy volunteers were randomized to receive a single intravenous injection of REGN5381 (0.3, 1, 3, 10, 30, or 100 mg) or placebo: 5–6 patients per active dose group and 16 patients treated with placebo. If four cohorts were enrolled, a standard deviation change in blood pressure of 8 mmHg would enable a minimum detectable difference of 7.7 mmHg (based on a 1-sided t-test at a significance level of 0.05).
Data exclusions	There were no data exclusions
Replication	Not applicable for clinical data.
Randomization	Participants were randomized 6:2 to receive single-dose intravenous REGN5381 (0.3, 1, 3, 10, 30, or 100 mg) or intravenous placebo.
Blinding	This is a double-blinded study. Study subjects, the investigators, and study site personnel were blinded to all randomization assignments throughout the study. The Sponsor Medical/Study Director, Study Monitor, and any other Regeneron personnel who were in regular contact with the study site will remained blinded to all subject randomization assignments.

Reporting for specific materials, systems and methods

We require information from authors about some types of materials, experimental systems and methods used in many studies. Here, indicate whether each material, system or method listed is relevant to your study. If you are not sure if a list item applies to your research, read the appropriate section before selecting a response.

Materials & experimental systems

n/a	Involved in the study
☐	☒ Antibodies
☐	☒ Eukaryotic cell lines
☒	☐ Palaeontology and archaeology
☐	☒ Animals and other organisms
☐	☒ Clinical data
☒	☐ Dual use research of concern
☒	☐ Plants

Methods

n/a	Involved in the study
☒	☐ ChIP-seq
☐	☒ Flow cytometry
☒	☐ MRI-based neuroimaging

Antibodies

Antibodies used

REGN5381 (Regeneron Pharmaceuticals, Inc.)
REGN2567 (Regeneron Pharmaceuticals, Inc.)
Mouse anti-his monoclonal antibody (Cytiva)

Validation

REGN5381 is a human immunoglobulin G4-based monoclonal antibody (developed by Regeneron Pharmaceuticals, Inc.) that binds and activates NPR1 in both the presence and absence of the endogenous ligands ANP and BNP. A high-throughput screen, VelocImmune® technology, was used to identify REGN5381. For additional information please visit: https://clinicaltrials.gov/ct2/show/record/NCT04506645

Eukaryotic cell lines

Policy information about cell lines and Sex and Gender in Research

Cell line source(s)

HEK293 from Human Embryonic Kidney

Authentication

Human 16-Marker STR Profile, Interspecies Contamination Test by IDEXX BioAnalytics (completed 11/9/2021). Identity match was shown to be >80%.

Mycoplasma contamination

Confirmed to be negative for mycoplasma - Tested by IDEXX BioAnalytics (completed by 9/30/2020)

Commonly misidentified lines
(See ICLAC register)

Name any commonly misidentified cell lines used in the study and provide a rationale for their use.

Animals and other research organisms

Policy information about studies involving animals; ARRIVE guidelines recommended for reporting animal research, and Sex and Gender in Research

Laboratory animals

The preclinical studies involved mice, beagle dogs and male cynomolgus monkeys (Macaca fascicularis)

Wild animals

The study did not involve wild animals

Reporting on sex

Sex-based analyses were not performed

Field-collected samples

Preclinical in vivo studies
NPR1hu/hu mice were generated on a C57BL/6NTac (75%)/129S6SvEvTac (25%) background using the Velocigene® platform. The generation of these mice was necessitated by the poor conservation of the NPR1 amino acid sequence between human and mouse, and the need to generate a human antibody. Each animal was implanted with PA-C10 (Data Sciences International, St. Paul, MN, USA) radiotelemetry devices for the recording of central arterial pressures. The transmitter was located in the carotid artery of each mouse. Mice were fed normal chow (PicoLab® Rodent Diet 20, #5001), housed under standard conditions, and allowed to acclimate for at least 7 days prior to being placed on study. REGN5381 was diluted with sterile phosphate-buffered saline for subcutaneous injection into mice.
Telemetered NPR1hu/hu mice were randomly assigned to one of five dosing groups (n = 4–7 per group) based on body weight, and received a single subcutaneous dose of saline or REGN5381 (1, 5, 25, or 50 mg/kg) on study day 0. The BP of each animal was continuously monitored for 28 days. Urine samples for urinalysis and urinary biomarkers were collected on day 28 post-dose.
Non-human primate studies
Thirty cynomolgus monkeys (Macaca fascicularis) of Mauritius origin, aged 2–4 years and weighing 3–5 kg (Charles River Laboratories, Inc., Reno, NV, USA), were enrolled for studies. For telemetry studies, each animal was implanted with PhysioTel Digital model L11 (Data Sciences International) radiotelemetry devices for recording the central arterial pressure and ECG waveforms. The transmitter was located intramuscularly in a dorsal position and lateral to the median plane below the ribs, and the attached BP catheter was located in the femoral artery with the tip of the catheter located in the descending aorta.
Animals were acclimated to laboratory housing for a minimum of 5 weeks before initiation of dosing (including recovery time after surgical implantation when performed). During treatment, non-human primates were housed individually in stainless-steel cages in a controlled environment under standard conditions. They were provided Purina Certified Primate Diet 5048 biscuits twice daily and assorted fresh fruit or vegetables. Reverse osmosis–filtered water was provided ad libitum by means of an automatic watering

system.
Dog telemetry study
Two beagle dogs (Canis lupus familiaris) aged 8-10 months and weighing 9–10.5 kg were received from Marshall BioResources (North Rose, NY) and enrolled in the study. For telemetry studies, each animal was implanted with PhysioTel Digital model D70 (Data Sciences International, St. Paul, MN) radiotelemetry devices for recording the central arterial pressure.
Animals were acclimated to laboratory housing for a minimum of 2 weeks before initiation of dosing (including recovery time after surgical implantation when performed). During treatment, dogs were housed in groups of two in a controlled environment under standard conditions. They were provided PMI Nutrition international, LLC Certified Canine LabDiet 5007 daily.
Acute anesthetized dog study
Twelve beagle dogs (Canis lupus familiaris) aged 11–13 months and weighing 9–15 kg were received from Covance (Cumberland, VA, USA) and enrolled in the study. General procedures for animal care and housing met current American Association for Accreditation of Laboratory Animal Care International recommendations, Guide for the Care and Use of Laboratory Animals and the U.S. Department of Agriculture through the Animal Welfare Act (as amended, and conformed to testing facility SOP)47-49. Dogs were housed in runs (up to two dogs per run). The temperature and humidity ranges of the study room were set to maintain 74 ± 10°F and 50 ± 20%, respectively. The light cycle was set to maintain 12 hours on/12 hours off. Dogs were offered Certified Canine Diet (LabDiet 5007) once daily except on the day of that dog's scheduled experiment; each dog was kept on an overnight fast before the day of its scheduled experiment. Dogs were provided fresh water ad libitum using an automatic watering system except when removed from the run. Anesthetized dogs were instrumented with venous and arterial catheters. Each dog received a single intravenous bolus dose of saline (control, n = 6) or 25 mg/kg REGN5381 (n = 6). Following dose administration, dogs were monitored for acute hemodynamic changes.

Ethics oversight

All mouse experiments were conducted in compliance with protocols approved by the Regeneron Pharmaceuticals Institutional Animal Care and Use Committee, in accordance with state and federal guidelines. All dog experiments were conducted in compliance with protocols approved by Charles River Labs or Battelle Institutional Animal Care and Use Committees. All nonhuman primate experiments were conducted in compliance with protocols approved by the Charles River Institutional Animal Care and Use Committee, in accordance with state and federal guidelines.

Note that full information on the approval of the study protocol must also be provided in the manuscript.

Clinical data

Policy information about clinical studies

All manuscripts should comply with the ICMJE guidelines for publication of clinical research and a completed CONSORT checklist must be included with all submissions.

Clinical trial registration

NCT04506645

Study protocol

Qualified researchers may request access to the study protocol at https://vivli.org/.

Data collection

Patient data was collated in a clinical setting, and study location including time period of recruitment and data collection is detailed on ClinicalTrials.gov.

Outcomes

Predefined Primary Endpoint
Here we present the first part study results. The primary endpoint in the study was the type, incidence, and severity of TEAEs following single IV dose administrations of REGN5381 or placebo over time in healthy normotensive and otherwise healthy hypertensive adults.

Predefined Secondary Endpoints
The secondary endpoints and assessments included:
• Change from baseline in SBP, DBP, mean arterial pressure (MAP), pulse pressure (PP), HR, and SV over time
• Maximum change from baseline in SBP, DBP, MAP, PP, HR, and SV across the first 24 hours postdose
• Change from baseline in the 24-hour mean SBP, DBP, MAP, PP, and HR measured from 0 to 24 hours, 24 to 48 hours, and 48 to 72 hours postdose
• Concentrations of REGN5381 over time
• Number and percentage of subjects who develop anti-drug antibodies (ADA) and titers over time

Predefined Exploratory Endpoints
The exploratory endpoints and assessment included:
• Change from baseline in urine cGMP and plasma cGMP over time
• Change from baseline in renin, aldosterone, N-terminal (NT)-proBNP and cardiac troponin T after dose administration over time
• Change from baseline in derivative of blood pressure over time (dP/dt)
• Change from baseline in urine output and sodium clearance over time
• Change from baseline in BP variability over time
• Change in SV, stroke volume variation (SVV), SBP, DBP, and MAP over time following a crystalloid fluid bolus

Flow Cytometry

Plots

Confirm that:

☐ The axis labels state the marker and fluorochrome used (e.g. CD4-FITC).

☐ The axis scales are clearly visible. Include numbers along axes only for bottom left plot of group (a 'group' is an analysis of identical markers).

☐ All plots are contour plots with outliers or pseudocolor plots.

☐ A numerical value for number of cells or percentage (with statistics) is provided.

Methodology

Sample preparation	Cells were suspended with enzyme free cell dissociation solution (Specialty Media, S-004-C) after rinsed with PBS once. The suspended cells were then collected with flow buffer (PBS supplemented with 2% FBS) and centrifuged. After removing supernatant, the cell pellets were resuspended and aliquoted 0.5 million cells in flow buffer into a 96-well plate (ThermoFisher Scientific, 249946) followed with a 30-minute incubation with primary antibody on ice. Cells were then incubated with Alexa Fluor 488- or APC-conjugated goat anti-human IgG secondary antibody (Jackson ImmunoResearch, 109-547-003 or 109-136-170) for 30 minutes on ice and viability dye staining (Invitrogen, L10120, or ThermoFisher Scientific, 65-0863-18) for 15 to 30 minutes on ice. Cells were washed twice with flow buffer or once with PBS post the secondary antibody staining or viability staining. The cells were then analyzed on a flow cytometer after centrifuged through a 96-well filter plate (PALL Corporation, 8027) into an U-bottom 96-well plate (Costar, 3360).
Instrument	CytoFlex Flow Cytometer, Beckman Coulter
Software	FlowJoTM 10, LLC Ashland, OR, USA
Cell population abundance	The final cell population was 25.9% to 64.0% of the total events.
Gating strategy	For measuring specific binding of REGN5381 to human and cynomolgus monkey NPR1, the cells were sequentially gated on lymphocytes (SSC-A vs FSC-A), viable cells, and single cells (FSC-H vs FSC-A). For measuring specific binding of REGN5381 to cNPR1, the cells were sequentially gated on lymphocytes (SSC-A vs FSC-A) and viable cells.

☐ Tick this box to confirm that a figure exemplifying the gating strategy is provided in the Supplementary Information.